ACTA TECHNICA JAURINENSIS
Vol. 16, No. 3, pp. 90-98, 2023
10.14513/actatechjaur.00697

Optimizing cutting fluid usage in cutting processes on CNC machines: A conceptual digital twin model for ecological sustainability

Milica Barać[1,*], Nikola Vitković[1], Dragan Marinković[1,2], Predrag Janković[1], Dragan Mišić[1]

[1]Faculty of Mechanical Engineering, University of Niš
Aleksandra Medvedeva 14, 18106 Niš, Serbia
[2]Department of Structural Mechanics and Analysis, Technische Universität Berlin
Country Strasse des 17. Juni 135, 10623 Berlin, Germany
*e-mail: milica.barac@masfak.ni.ac.rs

Submitted: 05/05/2023 Accepted: 27/05/2023 Published online: 14/06/2023

Abstract: The increasing demand for environmentally friendly manufacturing processes has led to the need for optimizing the use of cutting fluids in turning and milling processes. Cutting fluids are commonly used in cutting processes to reduce tool wear and improve cutting performance. However, cutting fluids have a negative impact on environment and human health. This paper proposes a conceptual model of an information system based on digital twin of the production process. This system will enable monitoring of the manufacturing process and provide a decision support system for helping industrial engineers manage its parameters. The model is represented by using SADT (Structured Analysis and Design Technique), and it is presented by using one of the most common problems of optimizing cutting fluid usage in cutting processes on CNC machines from an ecological perspective. The proposed model considers various cutting process parameters (cutting speed, feed rate, depth of cut) and cutting environment factors (cutting process temperature) to determine the optimal cutting fluid flow rate. To optimize the usage of cutting fluid, the smart information system acquires, processes, and stores data from cutting process temperature and cutting fluid flow sensors to establish the correlation between process parameters and sensor data, which is then used to develop a model. The proposed model can be integrated with existing CNC machines to reduce environmental impact while maintaining high productivity. This paper provides a promising approach for optimizing cutting fluid usage in CNC machining processes while promoting ecological sustainability.

Keywords: Cutting fluid optimization; Digital twin; SADT (Structured Analysis and Design Technique); Ecological sustainability; Sensors system

I. INTRODUCTION

Manufacturing industries have been a significant contributor to environmental degradation. The increasing demand for sustainable and eco-friendly manufacturing processes has become a crucial issue in recent years [1]. Machining processes such as turning and milling are widely used in the manufacturing industry. Cutting fluid (CF) is a type of coolant and lubricant designed specifically for metalworking and machining processes [2].

One of the significant challenges in machining processes is the optimization of CF usage. The cutting process heavily relies on CFs as crucial components. CFs are commonly used in turning and milling processes to reduce tool wear and improve cutting performance. During the cutting processes, CFs are vital in ensuring optimal cutting performance, prolonging tool life, preventing workpiece damage, enhancing surface quality, and boosting productivity [3]. However, the CFs usage has adverse effects on the environment, including water pollution, air pollution and the generation of hazardous waste.

CFs are one of the main causes of environmental pollution during the machining [4]. Therefore, the increasing demand for eco-friendly production methods due to environmental concerns has led to a growing interest in developing alternative methods for reducing the CFs usage while maintaining or improving machining performance. Also, CFs usage, in addition to a significant impact on the environment due to their composition and disposal, also leads to potential health risks and economic costs [5]. CF usage accounts for a substantial portion of production costs, averaging up to 17%, with only 6% attributed to the price of the fluid, and the remaining 94% to CF usage costs [6, 7].

The ultimate goal of eliminating CFs is often unattainable due to the stringent requirements of machining operations, making dry machining conditions not always a viable alternative [8]. Due to the adverse effects of CFs, it is essential to minimize their usage in cases where dry machining is not feasible. Minimizing CFs usage contributes to reducing environmental pollution, potential health risks to operators, and economic costs. To reduce the CFs usage and meet the aforementioned objectives, it is imperative to optimize the cutting process while ensuring that desired productivity and the final product quality are not compromised. This implies that the optimal usage of CFs is essentially the minimum amount required to satisfy the necessary surface quality and main machine time [9].

During machining operations, workpiece materials undergo plastic deformation that results in significant thermal stresses on both the cutting tools and workpieces [10]. To reduce the thermal stress that occurs, CFs are used. This means that the CFs usage is closely related to the heat generated in the cutting zone [11]. Therefore, when optimizing CF usage during cutting processes, it is essential to consider the heat generated, which necessitates the use of a temperature measuring sensor. To optimize the CFs usage, data from CF flow sensor and cutting process parameters are essential, in addition to temperature sensor data. Once all necessary data is gathered, filtered, and analysed, it leads to the correlation between the data that is used for developing an optimization model.

The integration of digital technologies into manufacturing processes has revolutionized the way production systems are managed and optimized. One promising approach is the utilization of digital twins. The escalating digitization of various aspects of daily life has resulted in increased opportunities for data acquisition, storage, transfer, and analysis, which has in turn fostered high expectations for the "Digital Twins" concept [12].

This paper introduces a conceptual model of an information system based on digital twin (DT) of manufacturing processes, specifically cutting. The information system is represented by using Structured Analysis and Design Technique (SADT). SADT is a comprehensive systems engineering and software engineering methodology employed for describing systems as a hierarchical arrangement of functions. The hierarchical structure enables the decomposition of the system into smaller parts and thus increases the detail of the system analysis. SADT is a graphical notation that is primarily intended to assist individuals in effectively describing and comprehending complex systems [13]. As the cutting process itself is very complex, SADT represents a good method for creating a conceptual model of an information system based on digital twin (DT) of cutting processes.

This paper presents a conceptual system that builds upon the authors' extensive experience in production engineering and workflow management. The conceptual model developed in this study serves as a crucial initial step in introducing a DT. The authors aim to transfer their knowledge and expertise into a novel workflow that enhances manufacturing processes by harnessing the power of real-time sensor(s) data. Central to this conceptual system is an information system model proposal that facilitates data acquisition and management. In the initial stage, expert knowledge will be leveraged to establish an expert system based on the user-expert experience in the manufacturing process. The main goal is to develop and propose a conceptual model of the intelligent information system that will enable different solutions to improve the manufacturing processes in clean manufacturing, process and product quality. The conceptual model of the information system is general, but to enable a better understanding of its possible applications, the focus will be on optimizing the usage of CFs in cutting processes on CNC machines, considering ecological sustainability.

II. Digital twins

Digital Twins (DTs) are becoming increasingly more important in research and industry as they offer significant benefits in the transition from traditional manufacturing to Smart Factories in line with Industry 4.0. DTs represent a multidisciplinary technology that harnesses the power of models, data, machines, and computers to deliver efficient, real-time, and intelligent services across various domains of smart manufacturing [14]. DTs have been widely adopted in the manufacturing industry to improve production efficiency and reduce costs. In recent years, DTs have been extended to environmental management, with applications in energy management and carbon footprint reduction.

When discussing DTs, it's important to consider their different integration levels: Digital Model (DM), Digital Shadow (DS), and full-fledged Digital Twin (DT) [15]. These levels represent varying degrees of data integration between the physical and virtual counterparts. The DM serves as a foundational virtual representation with geometric and static data. DS act as intermediaries, incorporating static and dynamic data for monitoring and analysis but lacking real-time control. Finally, the DT is a dynamic virtual replica closely mirroring the physical system in real-time, integrating various data sources and enabling real-time monitoring, control, and interaction.

Various definitions of DTs have been proposed by the scientific community with the goal of providing a consistent and comprehensive understanding of their diverse applications [16]. The absence of a universally accepted definition of DTs stems from their wide applicability across diverse industries, the rapidly evolving nature of the field, varying perspectives from different disciplines and communities, and the flexibility in implementation using different technologies and platforms. Overall, DT is a virtual model that replicates the physical characteristics and behaviour of a real-world object or system. They serve as an interface connecting the physical and information worlds [14].

The DT acquires and analyses data from its physical counterpart or other sources, using models and real-time and historical sensor data to assess the current state and predict future behaviour. By processing data, the DT generates recommendations, including optimization suggestions, which can be shared with users or integrated back into the physical system. The DT improves its own models by incorporating current data through a control loop, ensuring continuous refinement and adaptation to environmental changes for optimized results. DTs offer direct support to decision-making processes by providing specific recommendations or even acting autonomously [12]. The paper presents a conceptual model of a smart information system that utilizes a DT for decision-making.

III. SADT METHOD

SADT method is a diagramming technique that provides a graphical notation used in systems engineering for graphical modelling, description, and analysis of the structure of complex systems, their functions, and processes [13]. SADT, which can be applied to various systems comprising different components, enables analysis of their interrelated relationships. It offers a systematic approach to optimize machining processes by examining functions and activities involved. Widely used in software engineering and computer-aided manufacturing systems, SADT diagrams visually represent the system, aiding stakeholders in comprehending its behaviour and structure [13, 17-20].

In SADT, boxes and arrows are used as graphical symbols for constructing diagrams. Boxes represent processes, functions, actions, entities, or activities and contain brief descriptions. In SADT graphical notation, each box in the diagram is labelled in the lower right corner.

Arrows, in SADT graphical notation, have specific meanings:

- Inputs enter from the left, representing necessary data or consumables;
- Outputs exit to the right, indicating resulting data or products;
- Controls enter from the top, representing commands or conditions influencing the activity;
- Mechanisms enter from the bottom, signifying the means, components, or tools used to perform the activity and allocate activities.

SADT hierarchically represents complex systems, ensuring consistency and offering detailed information at each level. Breaking down systems allows analysts to identify issues and areas for improvement. Hierarchical SADT diagrams provide benefits such as clear representation, understanding of component interactions, and a framework for analysis, design, and testing.

IV. RESULTS AND ANALYSIS

The smart information system is a complex system representing a manufacturing environment workflow. The main components, which are the focus of this research, are data processing and decision support system. For data processing, DT is used to represent manufacturing processes and acquire real-time data using IoT, which is Industry 4.0 approach. The Decision Support system is an intelligent part of the information system focused on making decisions that will help industrial engineers resolve complex issues in the manufacturing environment. In the initial stage (concept), the decision support system will enable applying an expert system formed by using specialist knowledge, and an optimization model for finding the optimum of a defined process (CF in this case). Furthermore, machine learning will be applied to predict various solutions when enough sensor data is acquired in future work.

For this research, the information system will be demonstrated by applying SADT conceptual model of the cutting process on a CNC machine to optimize CF usage is hierarchical and consists of several levels of detail. This conceptual smart information system model is based on the authors' extensive experience in production engineering and workflow management. The highest level of the hierarchy depicts the system's overarching objective, which is further decomposed into constituent processes and sub-processes.

At the first level, the context diagram shows the overall smart information system that uses a DT of a process for decision-making. Overall SADT diagram of smart information system and its main inputs, outputs, resources/mechanisms and control elements is shown in **Fig. 1**.

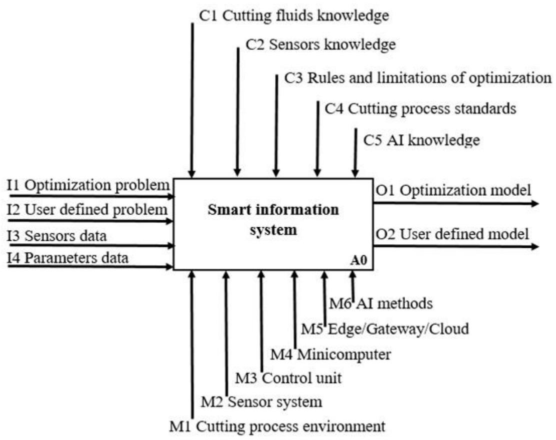

Figure 1. *Smart information system A0 - context diagram*

The system relies on essential data obtained through the use of resources, while considering established standards, rules, limitations and knowledge. In this stage, authors propose a conceptual information system model that utilizes real-time sensor data for data acquisition, serving as an initial step in introducing a DT. The following is a description of the element of the Smart information system for optimizing CF usage in CNC cutting process according to SADT specification.

Main inputs:

- Optimization (I1) and/or User Defined problem (I2) represents the main objective of the system, which is to optimize or to solve the cutting process. In this case, the focus will be on optimizing the usage of CFs, while ensuring that the quality of the final product and productivity are not compromised.
- Sensors data (I3) refers to the data obtained from the temperature and CF flow sensors, which provide information about the cutting process.
- Parameters data (I4) represents the cutting process parameters data, such as cutting speed, feed rate, and depth of cut, which are necessary for optimizing the cutting process.

Main resources/mechanism:

- Cutting process environment (M1) includes the cutting tool, workpiece, CNC machine and operator.
- Sensor system (M2) includes a CF flow sensor and an industrial temperature measurement sensor which gather data from the cutting process.
- Control Unit (M3) provides the necessary data on cutting process parameters such as cutting speed, feed rate and depth of cut.
- Minicomputer (M4) is a small computing device such as Raspberry Pi, Banana Pi, Arduino, or others that can be used to process data locally.
- Edge/Gateway/Cloud (M5) includes Edge, Gateway, and Cloud, and is used to store and analyse data.
- AI methods (M6) include proven techniques like Artificial Neural Network (ANN), Genetic Algorithm (GA), and others that have proven successful in similar optimization problems [21].

Main controls:

- CFs knowledge (C1) involves knowledge about the properties and characteristics of CFs and their effects on the cutting process.
- Sensors knowledge (C2) involves knowledge about the working principles of sensors used in the system.
- Rules and limitations of optimization (C3) involve rules and limitations that need to be considered during the optimization process, such as surface quality and main machine time requirements.
- Cutting process standards (C4) involve adhering to ISO standards and recommendations, such as temperature interval control, which provide guidance for optimization decisions.
- AI knowledge (C5) involves knowledge about applying AI methods to optimize the cutting process.

Main output:

- Optimization (O1) and/or User Defined Model (O2) in this case includes the optimized CF usage and ensures that the cutting process is sustainable, reducing the CF usage while maintaining the required processing quality and productivity. The model provides recommendations on the optimal cutting process parameters that will achieve the desired objective: minimizing CF usage without compromising production quality and productivity. The model should allow taking into account different criteria and different boundary conditions.

The decomposition process starts with the highest level of the SADT diagram, which is the context diagram, and progresses down through successive levels of detail. At the second level, the context diagram is decomposed into major processes with accompanying inputs, outputs, mechanisms, and control elements, with each process represented by a box, as shown in **Fig. 2**. Each process in SADT has its own label in the lower right corner of the box. The main processes represented in this first hierarchical decomposition step of the SADT diagram are Data processing (A1) and Decision support system (A2).

The process A1 - Data processing in the SADT diagram involves several steps to prepare and process the data obtained from the cutting process. During this process, the system acquires necessary data from sensors and control unit. This data is then processed and stored for later use. The purpose of this process is to ensure that the system has access to relevant and accurate data for optimization or

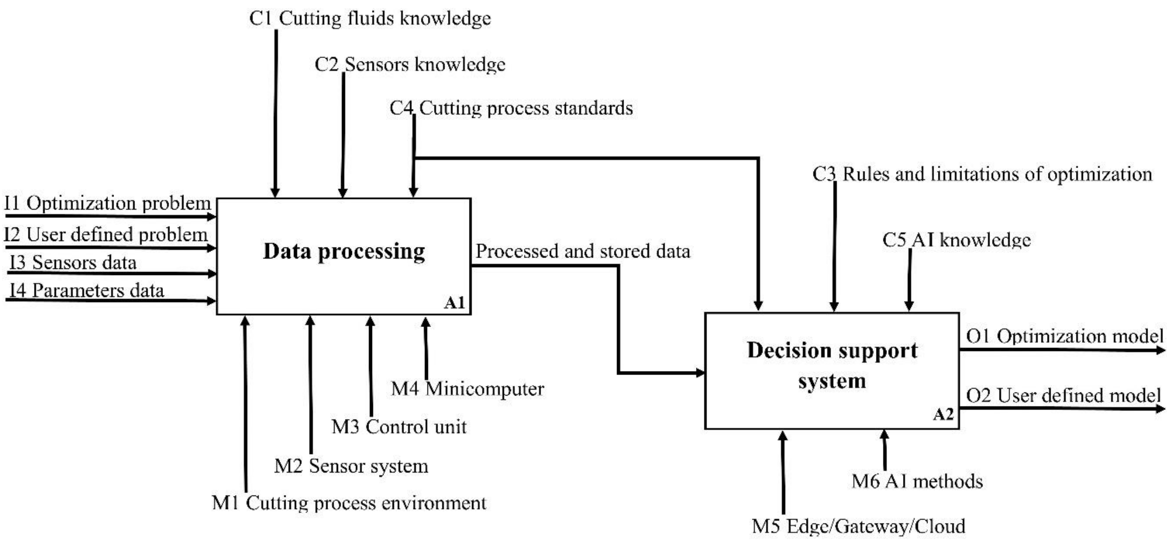

Figure 2. *Main processes of Smart information system – A0*

solving user defined problems. The processed and stored data represent the output of this process.

The process A2 - Decision support system is another main process in the SADT diagram that involves several steps for preparing and analysing the data that have been previously processed and stored locally. The output of the A1 process (processed and stored data) represents the input to this process. As part of this process, the system classifies and stores data on the cloud. Defined correlation between analysed data is used for developing optimization and/or user defined model. The model will be built to satisfy different objective functions and different boundary conditions. The decision support system serves to define optimal process parameters depending on and in accordance with optimization criteria and boundary conditions. Initially, this decision support system (expert system) based on expert knowledge will define a set of rules for analysing data and making preliminary decisions. Therefore, the expert system initially serves for process control and control of the optimization function to define the minimum value of CF usage. The knowledge required for this system will be acquired from specialists in academia and industrial engineering. In this process, depending on the case, optimization can be performed using optimization methods, or prediction can be applied using machine learning methods, or both. As more data is acquired, suitable AI methods will be applied.

Finally, at the third level, each process in the second level is decomposed further into sub-processes. The decomposition of the A1 process is shown on a separate SADT diagram in **Fig. 3**. The process A1 includes three sub-processes: Planning and preparation (A11), Data acquisition and processing (A12) and Data storage (A13). Each sub-process in SADT diagram is represented by a box with associated inputs, outputs, mechanisms and control elements (ICOM box).

The sub-process A11 - Planning and preparation involves defining the objectives, identifying the requirements, and planning the resources needed for data processing. During the planning and preparation sub-process, the system determines the data collection requirements and identifies the necessary sensors and equipment to be used as data sources. The aim of this sub-process is to ensure that data processing is properly planned and prepared before it begins, and that all necessary resources, including hardware and software tools, are available to execute the process efficiently and effectively. The output of this sub-process is a planned and prepared system for collecting the necessary data.

The sub-process A12 - Data acquisition and processing involves obtaining data from two sources and processing it to extract meaningful information. In order to eliminate superfluous data artefacts that are not pertinent to the analysis, such as noise, short circuits, and downtime, the data must undergo pre-processing. The system removes any errors or inconsistencies in the data during this sub-process. The control unit serves as the data source, providing information regarding the cutting process parameters such as cutting speed, feed rate, and depth of cut. The second data source is the sensor system, which includes an industrial temperature measurement sensor and a CF flow sensor. The system converts the raw data into a structured format suitable for storage and further analysis. The sub-process includes data validation, filtering, cleaning, and transformation. The goal is to ensure the collected data is accurate, reliable, and usable for subsequent analysis. The output of this sub-process is the acquired and processed data, which can be used for further analysis.

The sub-process A13 - Data storage involves securely and efficiently storing the processed data. The output of the A12 sub-process (acquired and processed data) serves as the input for this sub-

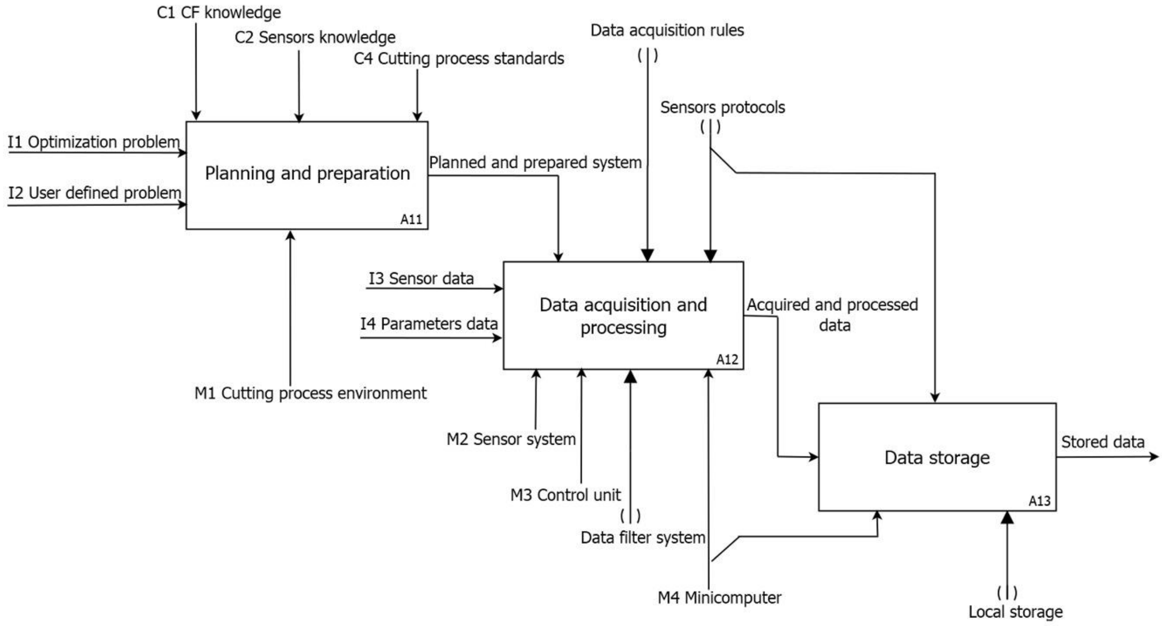

Figure 3. Sub-processes of Data processing – A2

process. The sub-process involves storing the acquired and processed data locally on external hard drive. The system ensures that the stored data is organized. This sub-process uses suitable storage techniques and data structures to store data in a structured file format, which can be easily accessed. The sub-process includes a strategy for backup and recovery in case of data loss. The primary purpose of this sub-process is to ensure that the processed data is both accessible and secure. The output of this sub-process is the locally stored data.

The decomposition of the A2 process is shown on SADT diagram in **Fig. 4**. The process A2 includes three sub-processes: Preparation of data for analysis (A21), Data analysis (A22) and Smart model development and application (A23). Each sub-process in SADT diagram is represented by an ICOM box.

The sub-process A21 - Preparation of data for analysis involves preparing the data for subsequent analysis on a cloud-based platform. The output from the main process A1, or more specifically from the sub-process A13 (stored data), represents the input to this sub-process. This sub-process involves receiving data and storing it in the cloud. The sub-process includes cleaning, transforming, and formatting the data to ensure that it is compatible with the cloud platform. Data transfer to the cloud is performed according to protocols and at specific intervals, unless there are any obstacles. If the connection to the cloud is interrupted for any reason, the data is still locally saved within the preceding A13 sub-process. Once the connection is restored, the data is transferred to the cloud. On the cloud, the data is classified, stored, and properly prepared in a suitable organized structure to be analysed. The purpose of this sub-process is to provide logically organized data on the cloud for further analysis. The output from this sub-process is prepared data for analysis.

The sub-process A22 - Data analysis involves analysing the prepared data. The purpose of this sub-process is to identify trends, anomalies, patterns, correlations, and insights within the data. The sub-process includes exploratory data analysis. The output of the A21 sub-process (prepared data) represents the input to this sub-process. This sub-process involves using various data analysis techniques to draw meaningful conclusions from the data. The use of various data analysis techniques allows to analyse large datasets in different ways and thereby identify complex correlations between process parameters. The primary objective of this sub-process is to obtain useful insights that can help optimize and solve problems in the cutting process environment. The output of this sub-process is a defined correlation between data.

The sub-process A23 - Smart model development and application involve the use of an expert system, optimization methods and AI methods, depending on the case and the amount of acquired data. This sub-process generates optimization recommendations or problem solutions that can be directed towards the user or integrated back into the physical system for real-time optimization and management. The goal is to define optimal cutting process parameters depending on various criteria and boundary conditions. In this case, primary objective is to optimize or solve the cutting process by reducing the usage of CF while ensuring that the quality of the final product and productivity are not compromised. The Smart model focuses on making decisions to solve complex challenges in the manufacturing process. Initially, the expert system will be used to

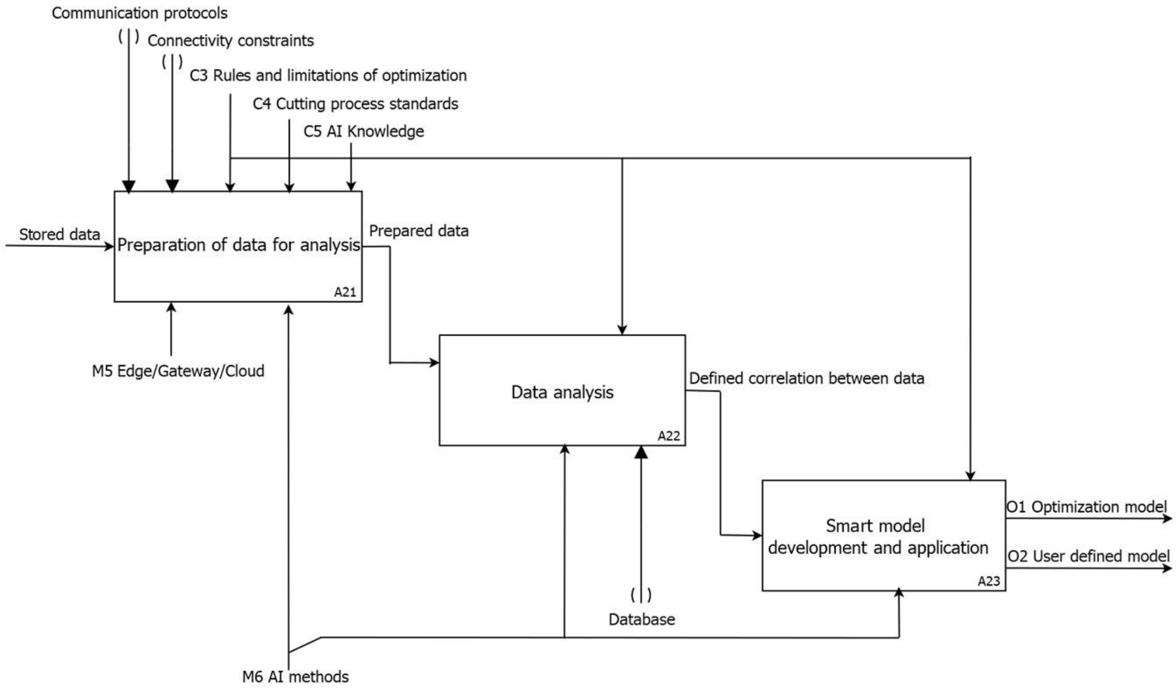

Figure 4. *Sub-processes of Decision support system – A2*

make preliminary decisions using predefined rules based on expert knowledge from academia and industry. Additionally, the optimization model will be applied to determine the optimal parameters for solving the defined optimization problem in the cutting process. As the research progresses, machine learning techniques will be used to predict and explore different solutions as a result of accumulating sufficient sensor data. The aim is to enhance the predictive capabilities of the system and further optimize the decision-making process in the production environment. The system is continuously improved, refining and adapting its own optimization and/or user defined models using an ever-increasing dataset, thereby increasing its maturity over time. The system provides direct support to decision-making processes by offering specific recommendations or even acting autonomously.

V. DISCUSSIONS

The conceptual system is based on the extensive authors experience in the field of production engineering and workflow management. The conceptual model is the first step in introducing DT, which will help authors transfer their knowledge into a novel workflow based on the sensors' real-time data. In this stage, authors propose an information system model that will be used for the data acquisition, and in the initial stage, expert knowledge will be used to form an expert system based on the user (expert) experience in manufacturing process. The conceptual model does not define any specific optimization or machine learning models, yet it presents the manufacturing process management system's overall structure, with the example of CF monitoring.

Initially, in the first stage of the information system application, an expert system (decision support system) will be used to define a set of rules which will be applied for analysing data and making initial decisions. The knowledge will be acquired from specialists from academia and industrial engineers. Then, an adequate AI method(s) will be applied when enough data is acquired, like the ones mentioned in [21]. To conclude, the smart part of the information system will be developed by applying different techniques based on the available data, and it will be a dynamic model, which means it will use various methods to establish adequate decisions. It will be constantly tested by using expert knowledge directly, or by an initially defined decision support system.

In summary, this paper focuses on the concept of an information system model as a foundation for implementing a DT within the manufacturing domain. By combining the authors' expertise, sensor-based real-time data, expert knowledge, and AI methodologies, the conceptual system aims to optimize and solve various optimization and/or user defined problems in manufacturing processes.

VI. CONCLUSIONS

In conclusion, the use of CFs is a major source of environmental pollution and health risks, and reducing their usage is a key priority for manufacturers. In machining processes where dry machining is not applicable, it is necessary to optimize the machining process to minimize the CF usage. That is why the focus is on solving this problem. This paper proposes a conceptual model of an information system based on digital twin (DT) of cutting processes with a focus on optimizing the CFs usage, considering ecological sustainability. The conceptual model proposed in this study was developed using the SADT methodology owing to its hierarchical decomposition. The conceptual system described in this paper is built upon the author's extensive experience in manufacturing engineering and workflow management.

The system aims to leverage digital twin technology and real-time sensor data to improve manufacturing processes. In the first step, data will be acquired, followed by making initial decisions using an expert system or an objective function (optimization). When enough data is acquired, machine learning will be applied to predict different solutions. The smart component of the information system will be dynamically developed using various techniques based on available data, continually tested with expert knowledge or an initially defined decision support system.

The conceptual model is aligned with the vision of cleaner production and sustainable development, and it offers a promising approach for optimizing CF usage in CNC machining processes. Considering that the conceptual model is general, it can also focus on solving other problems and needs of the process. The proposed model can be integrated with existing CNC machines to reduce environmental impact and improve worker safety, while also reducing costs associated with CF usage. Also, with different criteria, boundary conditions and objective functions, the system will be able to adapt and make decisions to solve various optimization and/or user defined problems in manufacturing processes. Overall, this paper highlights the importance of optimizing machining processes in line with environmental protection and demonstrates the potential of optimization models for achieving ecological sustainability in manufacturing.

The authors' global objective is to improve optimization and prediction accuracy using this system, and active efforts to achieve this will be undertaken in the forthcoming period.

Acknowledgement

This research was financially supported by the Ministry of Science, Technological Development and Innovation of the Republic of Serbia (Contract No. 451-03-47/2023-01/ 200109).

AUTHOR CONTRIBUTIONS

M. Barać: Conceptualization, Theoretical analysis, Writing, Review and editing.

N. Vitković: Conceptualization, Theoretical analysis, Review and editing, Supervision.

D. Marinković: Supervision.

P. Janković: Review and editing.

D. Mišić: Theoretical analysis.

Disclosure statement

The authors declare that they have no known competing financial interests or personal relationships that could have appeared to influence the work reported in this paper.

ORCID

Milica Barać https://orcid.org/0000-0002-5355-693X

Nikola Vitković https://orcid.org/0000-0001-6956-8540

Dragan Marinković https://orcid.org/0000-0002-3583-9434

Predrag Janković https://orcid.org/0000-0001-9951-4500

Dragan Mišić https://orcid.org/0000-0001-8765-3204

References

[1] D. Fratila, Environmentally friendly manufacturing processes in the context of transition to sustainable production, Comprehensive Materials Processing 8 (2014) pp. 163-175. https://doi.org/10.1016/B978-0-08-096532-1.00815-3

[2] M. M. Rahman, M. Hassan, M. Abdullah-Al Bari, An optimize system of using cutting fluid in machining operation for light work machine shop, International Journal of Engineering and Applied Sciences 4 (1) (2012) pp. 1-8. https://dergipark.org.tr/tr/download/article-file/217686

[3] S. Debnath, M. M. Reddy, Q. S. Yi, Environmental friendly cutting fluids and cooling techniques in machining: a review, Journal of cleaner production 83 (2014) pp. 33-47. https://doi.org/10.1016/j.jclepro.2014.07.071

[4] X. C. Tan, F. Liu et al., A decision-making framework model of cutting fluid selection for green manufacturing and a case study, Journal of Materials processing technology 129 (1-3) (2002) pp. 467-470. https://doi.org/10.1016/S0924-0136(02)00614-3

[5] A. Alok, S. Kumar, et al., Review on the effect of surface textured tool in the field of machining, Advances in Materials and Processing Technologies (2023) pp. 1-19.

https://doi.org/10.1080/2374068X.2023.2184580

[6] H. J. Heine, Dry Machining: A Promising Option, Foundry management & technology 126 (9) (1998) pp. 50-56.

[7] N. King, L. Keranen, et al., Wet versus dry turning: a comparison of machining costs, product quality, and aerosol formation, SAE Technical Paper (2001) 2001-01-0343. https://doi.org/10.4271/2001-01-0343

[8] E. Benedicto, D. Carou, E. M. Rubio, Technical, economic and environmental review of the lubrication/cooling systems used in machining processes, Procedia engineering 184 (2017) pp. 99-116. https://doi.org/10.1016/j.proeng.2017.04.075

[9] M. Barać, N. Vitković, M. Manić, Conceptual model of an information system for measuring cutting fluid temperature on CNC machines, in: J. Baralić, N. Dučić (Eds.), 38th International Conference of Production Engineering: ICPE-S 2021, University of Kragujevac, Faculty of Technical Sciences Čačak, Serbia, 2021, pp. 68-75. http://spms.fink.rs/doc/2021/Proceedings%20SPMS%202021.pdf

[10] C. G. Yuan, A. Pramanik, et al., Drilling of titanium alloy (Ti6Al4V)–a review, Machining Science and Technology 25 (4) (2021) pp. 637-702. https://doi.org/10.1080/10910344.2021.1925295

[11] T. H. C. Childs, K. Maekawa, P. Maulik, Effects of coolant on temperature distribution in metal machining, Materials science and technology, 4(11), (1988) pp. 1006-1019. https://doi.org/10.1179/mst.1988.4.11.1006

[12] F. Wilking, B. Schleich, S. Wartzack, Digital twins-definitions, classes and business scenarios for different industry sectors, in: Proceedings of the International Conference on Engineering Design (ICED21), Cambridge University Press, Gothenburg, Sweden, 1, 2021, pp. 1293-1302. https://doi.org/10.1017/pds.2021.129

[13] D. A. Marca, C. L. McGowan, SADT: Structured Analysis and Design Technique, McGraw-Hill Book Co., Inc.: New York, 1988.

[14] X. Liu, D. Jiang, et al., A systematic review of digital twin about physical entities, virtual models, twin data, and applications, Advanced Engineering Informatics, 55 (2023) 101876. https://doi.org/10.1016/j.aei.2023.101876

[15] W. Kritzinger, M. Karner, et al., Digital Twin in manufacturing: A categorical literature review and classification, in: M. Macchi, L. Monostori, R. Pinto (Eds.), 16th IFAC Symposium on Information Control Problems in Manufacturing INCOM 2018: IFAC (International Federation of Automatic Control) Proceedings Volume 51 (11), IFAC-PapersOnLine with Elsevier, Bergamo, Italy, 2018, pp. 1016-1022. https://doi.org/10.1016/j.ifacol.2018.08.474

[16] C. Bianconi, A. Bonci, et al., (2020, System thinking approach for digital twin analysis, in: 2020 IEEE International Conference on Engineering, Technology and Innovation (ICE/ITMC), IEEE, Cardiff, UK, 2020, pp. 1-7. https://doi.org/10.1109/ICE%2FITMC49519.2020.9198392

[17] D. T. Ross, K. E. Schoman, Structured Analysis for Requirements Definition, IEEE Transactions on Software Engineering, SE-3 (1) (1977) pp. 6-15. https://doi.org/10.1109/TSE.1977.229899

[18] F. Ahmed, S. Robinson, A. A. Tako, Using the structured analysis and design technique (SADT) in simulation conceptual modelling, in: A. Tolk, S. D. Diallo, I. O. Ryzhov, L. Yilmaz, S. Buckley, J. A. Miller (Eds.), Proceedings of the 2014 winter simulation conference, New York: IEEE, Savannah, GA, USA, 2014, pp. 1038–1049. http://doi.org/10.1109/WSC.2014.7019963

[19] M. E. Dickover, C. L. McGowan, D. T. Ross, Software design using: SADT, in: Proceedings of the 1977 annual conference (ACM '77). Association for Computing Machinery, New York, NY, USA, 1977, pp. 125–133. https://doi.org/10.1145/800179.810192

[20] D. T. Ross, Applications and Extensions of SADT, Computer, 18 (4) (1985) pp. 25-34. https://doi.org/10.1109/MC.1985.1662862

[21] M. Barać, N. Vitković et al., A review of machine learning methods applied in smart machining, in: M. Zdravković, M. Trajanović, Z. Konjović (Eds.), 12th International Conference on Information Society and Technology: ICIST 2022 Proceedings, Information Society of Serbia – ISOS, Belgrade, Serbia, 2022, pp. 244-246. https://www.eventiotic.com/eventiotic/files/Papers/URL/96770bc7-0fd1-442f-95f9-d2e805b598a2.pdf

ACTA TECHNICA JAURINENSIS
Vol. 16, No. 3, pp. 99-106, 2023
10.14513/actatechjaur.00698

Data-driven analysis of transport and weather impact on urban air quality

Bálint Csonka[1,*]

[1]Department of Transport Technology and Economics, Faculty of Transportation Engineering and Vehicle Engineering, Budapest University of Technology and Economics
Műegyetem rkp. 3., H-1111 Budapest, Hungary
*e-mail: csonka.balint@kjk.bme.hu

Submitted: 07/05/2023 Accepted: 22/05/2023 Published online: 14/06/2023

Abstract: Many cities face low air quality. To better predict the exceedance of air quality limits, the traffic's contribution to air pollution was analysed in this paper. Several studies used a twin site approach to determine the impact of urban traffic; however, it requires the deployment of stations at various locations. A time variant analysis to determine traffic's contribution and regression analysis were applied to determine the weather's impact. The results were validated using actual traffic data. It was found that the traffic's contributions to CO and NO_2 were 22 and 30%. It was noted that the seasonal fluctuation of NO_2 is significantly influenced by precipitation. Long-term trends of pollutants require further research.

Keywords: air quality; urban; traffic; weather; sustainability

I. INTRODUCTION

Since more and more people live in cities, the urban air quality has recently been a strong focus of researchers and media attention. Despite pollutant concentration limits set by legislation, air quality measurements show that concentrations frequently exceed the limit [1]. For example, 15, 34, and 4% of reporting stations registered exceedances of particulate matter with a diameter of 10 µm or smaller (PM_{10}), ozone (O_3) and nitrogen oxides (NO_X) annual limit values. Estimates of the health impact indicated that long-term exposures to PM_{10}, O_3, and NO_X in 2018 were responsible for 379 000, 19 400 and 54 000 premature deaths in EU 28, respectively [1].

Road traffic contributes to air pollution in various ways, including:

- **primary exhaust emission:** particulate matter and gases in engine exhaust,
- **secondary exhaust emission:** pollutants formed from primary exhaust emission,
- **non-exhaust emission:** wear of vehicle components, e.g., tyres [2].

In this paper, the focus is put on primary and secondary exhaust emissions. The vehicles' emission has been decreased significantly over the past decades. Despite these efforts, road transport is still an important source of PM, CO, and NO_X emission [3-5], contributing 10, 20 and 39%, respectively in 2018 in EU-28 countries [1]. Furthermore, the contribution of road transport to emission in dense urban areas may be significantly higher [6]. The sectors' contribution to O_3 concentrations was not calculated because O_3 is not emitted directly into the air but is created when volatile organic compounds and NO_X combine in the presence of sunlight.

To achieve real-world emission reduction, the European Union promotes clean mobility and requires each new passenger car model to pass the Worldwide Harmonized Light Vehicles Test Procedure (WLTP) [7]. Since local air pollution primarily affects urban areas, the identified research question are as follows: what reductions in road traffic emission can be expected from regulations and new technologies in urban areas? Furthermore, the difference between weekdays and weekends was put into focus to estimate how working from home may impact the total emission.

The structure of the paper is the following: after a brief literature review, the data and temporal twin site method are presented in Section 3. In Section 4, the results and discussion are given. Finally, the conclusions are drawn.

II. LITERATURE REVIEW

Air pollution was studied on various levels in the scientific literature. These studies mainly focus on PM, SO_2 and NO_X, but other components may emerge. On the atmospheric level, the transmission of air pollutants between countries was studied in several papers [8-9]. For example, a study emphasized the knowledge gaps and lack of data about the atmospheric transport of microplastics and its contribution to the worsening of air quality [10]. Other studies investigated the transmission of pollutants between cities [11-12]. For example, the effect of city-to-city air pollution transmission on COVID-19 health outcomes was investigated in [13]. It was found that $PM_{2.5}$, NO_2 and O_3 increase the number of infected people.

Since local emission contributes most of the total emission in the urban regions [14] other researchers studied local air pollution on a city scale. The issue has also attracted the attention of sensor developers who combined gas sensor arrays with machine learning in the E-nose concept using different materials to better fit the requirements [15]. Recently, traffic calming measures are introduced in many cities. Therefore, the relationship between traffic's emission and air quality was put in focus to support the evaluation of measures.

The corresponding studies are summarized in **Table 1**. To estimate the contribution of road traffic to local air pollution, characteristics of traffic was used. A study estimated the CO pollution based on total travelled distance and average speed using the Versit+ micro model as a reference in a small area [16]. Microscale traffic and related NO_X and PM_{10} emissions were simulated in a hot spot [17]. The effect of traffic characteristics on emission were analysed, but traffic's contribution to the total air pollution was not investigated. Accordingly, factors affecting air quality, such as weather, was not considered. A regional atmospheric chemistry model to quantify the NO_X emission from traffic was used in [18]. Beside traffic counts, the temperature, wind speed and mixing height were considered. It was noted that the model underestimated NO_X traffic emissions in urban areas on weekday between 6 AM and 5 PM. Similar underestimation of NO_X was found in other studies as well (e.g., [19-20]).

Another study aimed to analyse the influence of city-scale, traffic mode, and traffic congestion on $PM_{2.5}$ concentration [21]. The traffic was described by the number of buses and private cars, and the total length of the urban roads. It was found that congestion significantly increase the environmental effect of private car use. Close to our aims, the relationship between traffic volume and air pollution (NO_X, O_3) was modelled using COPERT traffic emission and WRF-Chem atmospheric chemistry model [22]. Despite factors affecting the air pollution, such as wind and peak temperature, were considered to minimize non-traffic-related emission, the model seriously underestimated the NO_X concentrations.

The contribution of road traffic to air pollution in several major cities was estimated in [23]. Data for daily pollution concentrations was 'deweathered' using a Random Forest model developed in [24] to isolate the trends. In absence of traffic volume data, measurement sites were categorized to estimate background pollution. Another study analysed the impact of traffic calming on air-quality in urban areas considering the wind [25]. It was found that

***Table 1.** Collected data in corresponding studies*

Study	*Weather*	*Traffic*	*Emission*
[16]	-	Travelled distance, speed	CO
[17]	-	Traffic volume, composition, speed	NO_X, PM_{10}
[18]	Wind, temperature, mixing height	Traffic volume	NO_X
[19]	Wind, temperature	Traffic volume	NO_X
[20]	Temperature, humidity, planetary boundary layer	Traffic volume	NO_X, CO_2, CO
[21]	Wind, planetary boundary layer	Number of vehicles, total road length	$PM_{2.5}$
[22]	Wind, temperature, cloudage	Traffic volume	NO_X, O_3
[23]	Wind, temperature, humidity [24]	-	mainly NO_2, PM
[25]	Wind	Traffic volume	$PM_{2.5}$
[26]	-	Traffic volume	NO_X
[27]	Precipitation	Traffic volume	$PM_{2.5}$, CO, NO_2, O_3

removing 100% of traffic reduces pollutants by less than 30% if the background concentration is considered. It was also shown that isolated measures have small impact on local air-quality and no impact on global emission in [26]. Besides weather and traffic data, the public perception to air-quality studies was introduced in [27] because public awareness and support are fundamental for air quality legislation and clean-air transitions [28]. It was found that public perception correlates more with traffic volume than actual air quality.

Based on the literature review, it was found that many studies investigated the relationship between weather, traffic, and air-quality. Yet, emission is often underestimated. In the literature, time variant analysis can be found, but the traffic's contribution usually not determined for various periods [29]. Furthermore, Budapest, Hungary region lacks a comprehensive study about the status and long-term trends of key air pollutants, which is also a novelty of this paper.

III. Data and method

In this study, air-quality, weather, and traffic volume data were used. Publicly available data about air quality collected between 2008 and 2019 by automated air-quality monitoring stations were used. The measurements were performed in each hour. The stations are operated by the Ministry of Agriculture (levegominoseg.hu). There are 12 stations in Budapest and 7 stations were selected for analysis because of the high availability in the investigated period. The ministry categorized the stations into two groups based on the distance between the station and major roads: urban background and urban traffic. Urban traffic air-quality monitoring stations are close to the major roads. Data about the following pollutants were collected: CO, NO_2, O_3, and PM_{10}.

Publicly available data about weather collected by the Hungarian Meteorological Service (met.hu) were used. Data about the lowest, median, and highest temperature and precipitation on each day between 2008 and 2019 were used. Data about sunshine duration were available until 2013, and data about wind is available from 2011.

Traffic volume data at junctions and along an urban highway were used. Data about hourly traffic volume at junctions were provided by the Centre of Budapest Transport (bkk.hu). In this study, 6 high traffic junctions were selected based on the distance between junctions and air-quality monitoring stations. Publicly available data about daily average traffic volume on urban highway were given by Hungarian Public Roads (kozut.hu) for each month. Since the organization focuses on national roads, only 1 measured section is in Budapest. Hourly and monthly traffic volume data were used to analyse the relationship between traffic and air quality on different time horizons. Publicly available data about the congestion level in Budapest were provided by tomtom (tomtom.com). Monthly congestion level values were available for 2019.

The locations of air-quality monitoring stations and traffic volume counting are given in **Fig. 1**. Stations 2, 4 and 7 are in the urban background group. The urban highway traffic volume was measured at B. In Budapest, there are no significant industrial emission sources.

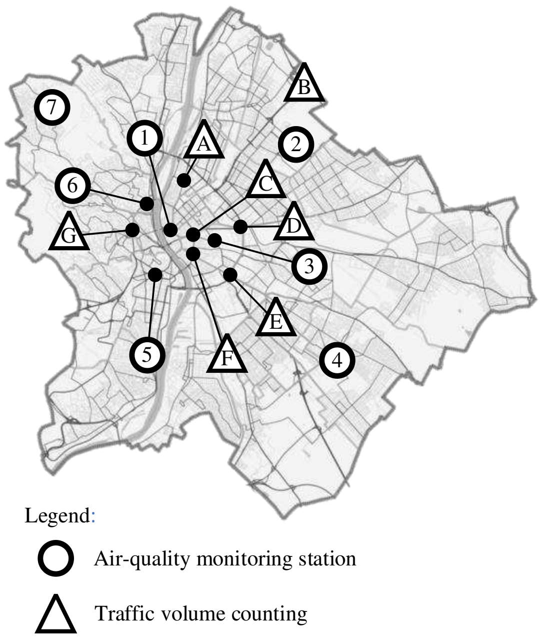

Figure 1. *Locations of air-quality monitoring stations and traffic volume counting*

Several studies apply the twin site approach to determine the contribution of traffic to air pollution. In this case, one of the air quality monitoring stations is along a major road, and the other one is far away. In this study, the considered monitoring stations are close to each other, and no significant difference could be observed regarding the NO_2 concentration characteristics. The average monthly NO_2

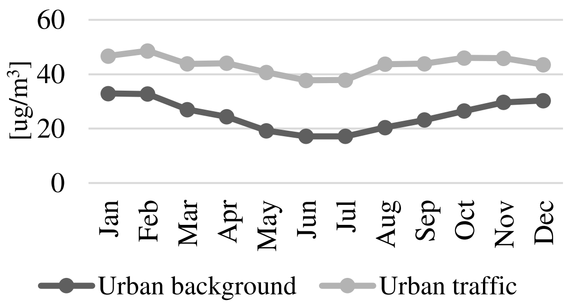

Figure 2. *Average NO_2 concentration between 2008 and 2019*

concentration at urban background and urban traffic stations are given in **Fig. 2**.

Therefore, twin site analysis was performed in time. The measurements were divided into two groups: weekdays and weekends. The hypothesis was that the difference between hourly average emission on weekdays and weekends reflects the emission of traffic. However, in this way, the emission will be underestimated by the weekend traffic. Based on traffic counting, average weekend traffic is appr. 45% of the weekday traffic. Accordingly, the weekday and weekend emissions were 180% and 80% of the difference between weekend and weekday concentration. The same rate was applied for each air-quality monitoring station group, and the subtraction was performed for each month. A strong correlation between CO and PM_{10} was found at each station. Therefore, the two were analysed together. Namely, it was assumed that they have a common source. This is in line with the fact that heating is a significant source of CO and PM_{10}.

IV. RESULTS AND DISCUSSION

The average difference between weekday and weekend emissions in December for urban traffic and urban background stations is presented in **Fig. 3**. Similar characteristics were found in each month. The difference reflects the daily traffic fluctuation, which validates the method. The higher peaks and valley between the peaks can be seen at the urban traffic stations, which is in line with Budapest's traffic characteristics. Traffic contribution to NO_2 concentration was determined for weekdays and weekends in each month (**Table 2.**).

Our results show that traffic regulation may significantly impact air quality in August and September. According to the differences between weekdays and weekends, working from home may decrease traffic's contribution by 16%. Since the main source of O_3 is NO_2, it was assumed that the traffic's contribution to O_3 emission is the same.

A similar analysis was performed to determine the traffic's impact on CO and PM_{10} concentrations. The average difference between weekday and weekend emissions in December for urban traffic and urban background stations is presented in **Fig. 4**. Similar characteristics were found in each month. It is noted that the weekend emission is significantly higher between 0 AM and 4 AM during the cold months and lower during daytime because of lower traffic. The two phenomena balance each other causing a low contribution of traffic. Accordingly, this method may be used with limitations for pollutants with low traffic contribution.

Table 2. *Contribution of traffic to NO_2 concentration*

Month	***Urban traffic station***		***Urban background station***	
	Mo-Fr	***Sa, Su***	***Mo-Fr***	***Sa, Su***
Jan	34%	19%	37%	21%
Feb	34%	19%	37%	20%
Mar	22%	11%	34%	18%
Apr	34%	19%	42%	25%
May	22%	11%	32%	17%
Jun	36%	20%	42%	24%
Jul	31%	17%	43%	25%
Aug	41%	24%	56%	36%
Sep	35%	19%	49%	30%
Oct	17%	8%	26%	14%
Nov	31%	16%	44%	26%
Dec	23%	12%	26%	14%

Legend:
Mo-Fr: Monday-Friday
Sa, Su: Saturday and Sunday

Furthermore, it indicates that home office in cold months may not decrease the total emission because the impacts of increased heating and lower traffic are roughly equal. To mitigate this effect on traffic CO emission, the lowest value was subtracted before multiplication and was added after multiplication.

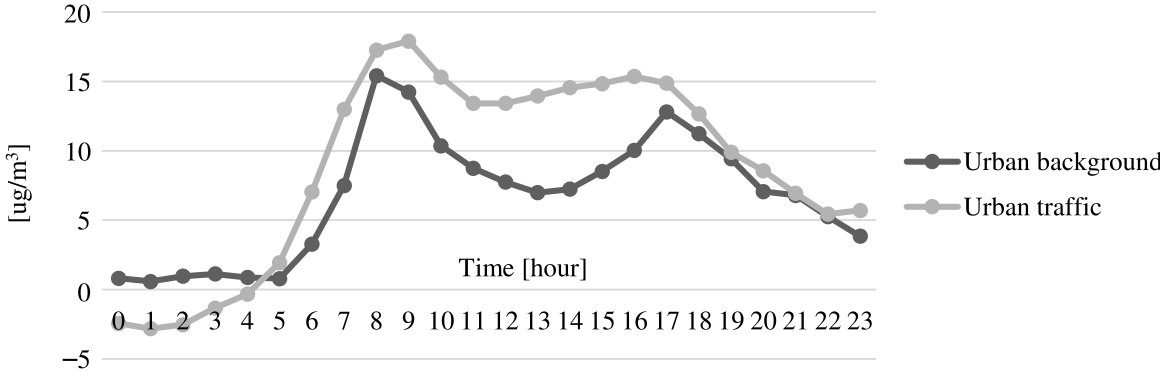

Figure 3. *The average difference between weekday and weekend NO_2 emissions in December*

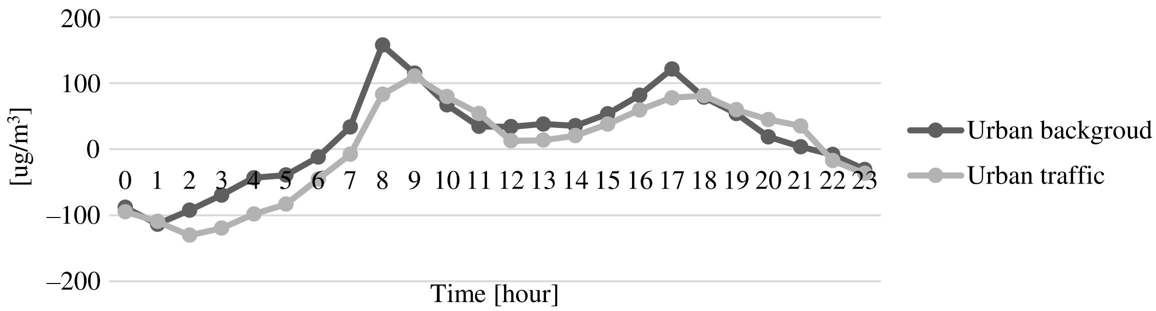

Figure 4. *The average difference between weekday and weekend CO emissions in December*

The contribution of traffic to CO emission on weekdays and weekends is summarized in **Table 3**. It is noted that the traffic's contribution on weekends is negligible. The difference between weekday and weekend emission characteristics reflects the differences in emission of other sources as well. It was assumed that the PM_{10} contribution is similar, which is in line with the results in [5], which estimated that the traffic's contribution is between 10% and 30%.

The average monthly traffic contribution for NO_2 and CO are summarized in **Table 4**.

The average contribution NO_2 was 30%. This is significantly lower than what was found in [30], which may be because of the vehicle technology developments and the higher distance between the road and the monitoring stations. However, it is greater than the estimated traffic's contribution (21%) was in Budapest in 2012 [31]. The average contribution CO was 22%. The contribution was the lowest in January and October and low in the cold months. CO concentration usually exceeds the limit during winter when traffic regulation cannot cause a significant decrease. Therefore, the heating system should be improved.

Table 3. *Contribution of traffic to CO concentration*

Month	*Urban traffic station*		*Urban background station*	
	Mo-Fr	***Sa, Su***	***Mo-Fr***	***Sa, Su***
Jan	14%	0%	17%	2%
Feb	28%	6%	26%	6%
Mar	20%	0%	21%	1%
Apr	32%	6%	31%	4%
May	29%	3%	26%	1%
Jun	40%	7%	31%	2%
Jul	44%	8%	37%	4%
Aug	46%	10%	36%	4%
Sep	49%	13%	35%	6%
Oct	18%	0%	17%	–1%
Nov	24%	4%	27%	6%
Dec	31%	9%	26%	6%

Legend:
Mo-Fr: Monday-Friday
Sa, Su: Saturday and Sunday

Table 4. *Average contribution of traffic to NO_2 and CO concentration*

Month	*NO_2*	*CO*
Jan	31%	11%
Feb	31%	21%
Mar	24%	15%
Apr	34%	24%
May	23%	20%
Jun	34%	20%
Jul	33%	31%
Aug	44%	31%
Sep	37%	33%
Oct	19%	12%
Nov	33%	20%
Dec	21%	23%

The seasonal fluctuations of NO_2 and CO were analysed. A relationship between traffic volume, precipitation and NO_2 concentration was found and the emission using linear regression was calculated (eq.1).

$$E_{NO2} = 28.97 + 0.362Cl - 2.808P \qquad (1)$$

Where E_{NO2} is the average NO_2 concentration [ug/m^3], Cl is the congestion level calculated by

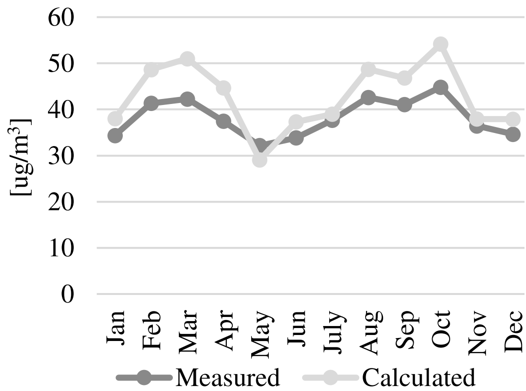

Figure 5. *Measured and calculated NO_2 emissions in 2019*

tomtom [%], and *P* is the average precipitation [mm]. R^2 is equal to 0.55. Therefore, further analysis is recommended, but data about monthly traffic were only available for 2019. Measured and calculated NO_2 concentration values are given in **Fig. 5**.

In the case of CO and PM_{10}, a strong correlation was found with the median temperature: the coefficients were between –0.91 and 0.95 at each station. Finally, the long-term trends of NO_2 and CO were analysed. No significant relationship was found between NO_2 and average traffic volume over the years. It may be because other factors cover the effect of higher traffic volume. Therefore, further analysis is required. In the case of CO, a correlation between CO and the median temperature was found in the cold months and between CO and precipitation during summer.

V. Conclusions

Analysis of traffic's contribution to air pollution helps forecast air quality and determine effective measures. In this study, the traffic's contribution was calculated using time variant analysis to determine the difference between weekday and weekend emission, which is the paper's main contribution. The results were validated using real-world traffic data. The average CO and NO_2 emissions contributions were 22 and 30%, respectively. According to the results, traffic regulations are the most effective during summer in the term of air pollution. Accordingly, improving other sources, such as the heating system, helps reduce exceedances of air quality standards. Seasonal analysis revealed that NO_2 concentration is strongly influenced by precipitation. It was noted that home office may not decrease the total CO pollution in cold months It was also found that CO correlates with PM_{10} and median temperature over the year. In the case of long-term trends, it was found that CO correlates with precipitation during summer, and NO_2 does not correlate with traffic. It may be because the annual traffic data was measured on a highway. Accordingly, further research about seasonal and long-term trends is necessary to predict air quality better.

Author Contributions

B. Csonka: Conceptualization, methodology, analysis, visualization, writing—review and editing.

Disclosure Statement

The authors declare that they have no known competing financial interests or personal relationships that could have appeared to influence the work reported in this paper.

ORCID

B. Csonka https://orcid.org/0000-0002-4976-8294

References

[1] EEA, Air quality in Europe – 2020 report (2020) https://doi.org/10.2800/786656

[2] F. Amato, F.R. Cassee et al., Urban air quality: The challenge of traffic non-exhaust emissions, Journal of Hazardous Materials 275 (2014) pp. 31-36. https://doi.org/10.1016/j.jhazmat.2014.04.053

[3] M. Guarnieri, J.R. Balmes, Outdoor air pollution and asthma, The Lancet 383 (2014) pp. 1581-1592. https://doi.org/10.1016/S0140-6736(14)60617-6

[4] W. Chen, A. Li, F. Zhang, Roadside atmospheric pollution: still a serious environmental problem in Beijing, China, Air Quality, Atmosphere & Health 11 (2018) pp. 1203-1216. https://doi.org/10.1007/s11869-018-0620-2

[5] S. Paraschiv, L.S. Paraschiv, Analysis of traffic and industrial source contributions to ambient air pollution with nitrogen dioxide in two urban areas in Romania, Energy Procedia 157 (2019) pp. 1553-1560. https://doi.org/10.1016/j.egypro.2018.11.321

[6] C. A. Belis, F. Karagulian et al., Critical review and meta-analysis of ambient particulate matter source apportionment using receptor models in Europe, Atmospheric Environment 69 (2013) pp. 94-108. https://doi.org/10.1016/j.atmosenv.2012.11.009

[7] ICCT Briefing, On the Way to "Real-World" CO_2 Values: The European Passenger Car Market in its First Year After Introducing the WLTP (2020).

[8] S. Itahashi, I. Uno et al., Nitrate transboundary heavy pollution over East Asia in winter. Atmospheric Chemistry and Physics 17 (2017) pp. 383-3843. https://doi.org/10.5194/acp-17-3823-2017

[9] S. Chen, T. Yuan et al., Dust modeling over East Asia during the summer of 2010 using the WRF-Chem model, Journal of Quantitative Spectroscopy and Radiative Transfer 213 (2018) pp. 1-12. https://doi.org/10.1016/j.jqsrt.2018.04.013

[10] S. Sridharan, M. Kumar et al., Microplastics as an emerging source of particulate air pollution: A critical review, Journal of Hazardous Materials 418 (2021) p. 126245. https://doi.org/10.1016/j.jhazmat.2021.126245

[11] X. Fu, Z. Cheng et al., Local and Regional Contributions to Fine Particle Pollution in Winter of the Yangtze River Delta, China, Aerosol and Air Quality Research 16 (2016) pp. 1067-1080. https://doi.org/10.4209/aaqr.2015.08.0496

[12] Y. Wang, Y. Li et al., Inter-city air pollutant transport in The Beijing-Tianjin-Hebei urban agglomeration: Comparison between the winters of 2012 and 2016, Journal of Environmental Management 250 (2019) p. 109520. https://doi.org/10.1016/j.jenvman.2019.109520

[13] S.A. Sarkodie, P.A. Owusu, Global effect of city-to-city air pollution, health conditions, climatic & socio-economic factors on COVID-19 pandemic, Science of The Total Environment 778 (2021) p. 146394. https://doi.org/10.1016/j.scitotenv.2021.146394

[14] Y. Wang, S. Bao, Local and regional contributions to fine particulate matter in Beijing during heavy haze episodes, Science of The Total Environment 580 (2017) pp. 283-296. https://doi.org/10.1016/j.scitotenv.2016.12.127

[15] L. Mahmood, M. Ghommem, Z. Bahroun, Smart Gas Sensors: Materials, Technologies, Practical Applications, and Use of Machine Learning – A Review, Journal of Applied and Computational Mechanics 9 (3) (2023) pp. 775-803. https://doi.org/10.22055/JACM.2023.41985.3851

[16] A. Csikós, T. Tettamanti, I. Varga, Macroscopic Modeling and Control of Emission in Urban Road Traffic Networks, Transport 30 (2015) pp. 152-161. https://doi.org/10.3846/16484142.2015.1046137

[17] C. Quaassdorff, R. Borge et al., Microscale traffic simulation and emission estimation in a heavily trafficked roundabout in Madrid (Spain), Science of the Total Environment 566–567 (2016) pp. 416-427. https://doi.org/10.1016/j.scitotenv.2016.05.051

[18] F. Kuik, A. Kerschbaumer et al., Top–down quantification of NO_X emissions from traffic in an urban area using a high-resolution regional atmospheric chemistry model, Atmospheric Chemistry and Physics 18 (2018) pp. 8203-8225. https://doi.org/10.5194/acp-18-8203-2018

[19] J.D. Lee, C. Helfter et al., Measurement of NO_X Fluxes from a Tall Tower in Central London, UK and Comparison with Emissions Inventories, Environmental Science & Technology 49 (2015) pp. 1025-1034. https://doi.org/10.1021/es5049072

[20] T. Karl, M. Graus et al., Urban eddy covariance measurements reveal significant missing NO_X emissions in Central Europe, Scientific Reports 7 (2017) p. 2536. https://doi.org/10.1038/s41598-017-02699-9

[21] J. Lu, B. Li et al., Expansion of city scale, traffic modes, traffic congestion, and air pollution, Cities 108 (2021) p. 102974. https://doi.org/10.1016/j.cities.2020.102974

[22] A. Kovács, Á. Leelőssy et al., Coupling traffic originated urban air pollution estimation with an atmospheric chemistry model. Urban Climate 37 (2021) p. 100868. https://doi.org/10.1016/j.uclim.2021.100868

[23] R.M. Harrison, T. Vu et al., More mileage in reducing urban air pollution from road traffic, Environment International 149 (2021) p. 106329. https://doi.org/10.1016/j.envint.2020.106329

[24] T.V. Vu, Z. Shi et al., Assessing the impact of clean air action on air quality trends in Beijing using a machine learning technique, Atmospheric Chemistry and Physics 19 (2019) pp. 11303-11314. https://doi.org/10.5194/acp-19-11303-2019

[25] H. Wang, P. Brimblecombe, K. Ngan, A numerical study of local traffic volume and air quality within urban street canyons, Science of the Total Environment 791 (2021) p. 148138. https://doi.org/10.1016/j.scitotenv.2021.148138

[26] D. Rodriguez-Rey, M. Guevara et al., To what extent the traffic restriction policies applied in Barcelona city can improve its air quality? Science of the Total Environment 807 (2) (2022) p. 150743. https://doi.org/10.1016/j.scitotenv.2021.150743

[27] H. O'Leary, S. Parr, M. M.H. El-Sayed, The breathing human infrastructure: Integrating air quality, traffic, and social media indicators, Science of The Total Environment 827 (2022) p. 154209. https://doi.org/10.1016/j.scitotenv.2022.154209

[28] J. Liang, P. He, Y. Qiu, Energy transition, public expressions, and local officials' incentives: Social media evidence from the coal-to-gas transition in China, Journal of Cleaner Production 298 (2021) p. 126771. https://doi.org/10.1016/j.jclepro.2021.126771

[29] L. Makra, H. Mayer et al., Variations of traffic related air pollution on different time scales in Szeged, Hungary and Freiburg, Germany, Physics and Chemistry of the Earth 35 (2010) pp. 85-94. https://doi.org/10.1016/j.pce.2010.03.005

[30] S. R. Gadsdon, S. A. Power, Quantifying local traffic contributions to NO_2 and NH_3 concentrations in natural habitats, Environmental Pollution 157 (10) (2009) pp. 2845-2852. https://doi.org/10.1016/j.envpol.2009.04.010

[31] I. Sundvor, N.C. Balaguer et al., Road traffic's contribution to air quality in European cities, ETC/ACM (2012)

ACTA TECHNICA JAURINENSIS
Vol. 16, No. 3, pp. 107-115, 2023
10.14513/actatechjaur.00690

Analysis of Truck Crashes with W-beam Guardrail

Tran Thanh Tung [1,*], Tso-Liang Teng [2]

[1] Faculty of Engineering Mechanics and Automation, VNU University of Engineering and Technology, 144 Xuan Thuy - Cau Giay District , Hanoi, Vietnam
[2] Department of Mechanical Engineering, Hsiuping University of Science and Technology, No.11, Gongye Rd., Dali Dist., Taichung City 412, Taiwan
*e-mail: tranthanhtung@vnu.edu.vn

Submitted: 16/03/2023 Accepted: 10/05/2023 Published online: 07/07/2023

Abstract: W-beam guardrail is an excellent method for enhancing traffic safety. The W-beam guardrail comprises of a W-shaped segment and specialized constructions known as support posts. Identifying the effect of the W-beam heights, post spacing, shaped supporting posts, and post-soil interaction may be crucial to improving the crashworthiness of W-beam guardrail. This study evaluated the W-beam guardrail using a finite element model in the event of a 10,000 kg truck collision. Simulations of crash tests were conducted to evaluate the crashworthiness of the W-beam guardrail in accordance with European standard EN1317. The results of this analysis can assist evaluate the design of W-guardrails and guide the future development of guardrail technologies.

Keywords: crashworthiness; W-beam guardrail; simulation; EN1317; LS-DYNA

I. INTRODUCTION

Off-road vehicle accidents occur when drivers lose control of their vehicles or veer to avoid the roadside hazard. As a result, the car could crash into other vehicles, pedestrians, or objects. These crashes could result in serious injuries or even death [1-8].

The W-beam guardrail is installed on the roadway to protect vehicles from roadside hazards and providing a high level of safety in and after the collision. Usually, the W-guardrail consists of a metal W-shaped segment and a supporting post, as shown in **Fig. 1**.

Figure 1. *W-beam guardrail [8]*

W-beam guardrails are an effective solution to reduce the risk of injury, save lives, and ensure road safety in the event of an accident. Previous research's indicate that the number of fatalities resulting from collisions with roadside guardrails was less than that resulting from collisions with other roadside hazards (trees, embankments, etc.) [9-11]. Thus, W-beam guardrails have proven an effective solution to reduce harm to cars and people when a collision occurs [12-14].

Usually, the W-beam guardrail must fulfil the European standard EN1317. The standards offer crash test details between multiple vehicle types with road safety W-beam guardrails. In addition, each W-beam guardrail must pass normalized crash tests according to established standards [15-16].

There were many studies which have been undertaken to investigate the capacity of W-beam guardrail based on European standard EN1317. Atahan et.al [17] shown a series of experimental impact test to determine the crashworthiness of the W-beam guardrail. In their study, Matthew Gutowski [18] proposed a new W-beam guardrail structure using the simulation method. Matej et al. [19] presented a steel-reinforced wooden W-beam guardrail design tested according to the EN1317 standard. Many researchers [20-23] provided an overview of the behavior of crashworthiness of roadside W-beam guardrail with different designs. Ferdous et al. [24] performed simulations with variable guardrail vehicle impact heights with W-beam guardrail. Lee et al. [25] evaluated the automotive crash performance of W-Beam steel post flexible rails in sloping ground supported with three types of cylinder shapes.

Normally, The W-beam guardrail structure was made to have certain dimensions, including the height from the ground surface and the distance between two posts [26–28]. In general, the installation of W-beam guardrails on European highways uses many shaped supports [29-30]. In addition, the W-guardrail guardrail is usually installed in a certain terrain where the poles will be embedded into the ground at a certain depth. W-beam guardrails can be installed on stable ground, asphalt, or concrete [11] [31-32]. Therefore, the influence of the soil on the posts an important factor in the safety performance of the W-beam guardrail, because the W-guardrail guardrail is often installed on different locations. As mentioned above, rail heights, post spacing, supporting posts, and post-soil were important factors affecting in safety performance of W-beam guardrails. Therefore, it was necessary to understand the influence of these parameters on safety performance. In the previous researches, Teng et al. [33-36] apply the finite element method to estimate the safety performance of W-beam guardrail, in which a 900 kg car crashes with W-beam guardrail (TB11-impact speed and impact angle were set 100 km/h and 200, respectively) in different rail height, post spacing, and post-soil interaction. The finite element approach was used to determine the safety performance of the W-beam guardrail constructed for varied structures: height and spacing of post, soil qualities, and shaped posts when impacted by a truck. The analytical results obtained here can help evaluate W-beam guardrail design and guide the future development of guardrail technologies.

II. W-BEAM GUARDRAIL AND EUROPEAN STANDARD EN 1317

1. W-beam guardrail

W-beam guardrail is the most commonly specified road safety barrier device in the world to protect vehicles and drivers from hazardous road places. **Fig. 2** depicts a typical W-beam guardrail, which consists of a W-shaped structure called a w-beam and specifically constructed posts. The W-beam guardrail absorbs a portion of the impact energy to lessen the risk to the driver and restrict vehicle deformation.

Figure 2. *Typical W-beam guardrail [8]*

2. European standard EN 1317

Typically, W-beam guardrails were constructed employing severity (ASI, THIV) and working width in accordance with European standard EN 1317-2 [15]. These standard tests depict conventional vehicle vs W-beam guardrail collision testing. The W-beam guardrail was built in accordance with the European standard EN 1317, taking into account three primary criteria for difference performance levels: containment level, impact severity, and working width.

Containment level: this represents the level of road safety barriers for various accident situations in terms of vehicle type, angle of impact, and impact speed. There were four containment levels from low to very high were specified.

Impact severity was characterized by the acceleration severity index (ASI) and the theoretical head impact velocity (THIV). To ensure safety, the following requirements must be met: ASI $\leq$ 1.0 (level A), $1<ASI\leq1.4$ (level B), $1.4<ASI\leq1.9$ (level C) and THIV$\leq$33 km/h.

Barrier deformation (Wm)) is regarded as the barrier's maximum lateral deformation with eight classes (W1–W8) were defined.

III. SIMULATION MODELS OF IMPACT TEST

In this study, simulations of TB42 type crash tests for heavier vehicles were performed to investigate the crashworthiness of different W-beam guardrail structures. This model consists of the truck (10,000 kg) with the W-beam guardrail according to the TB42 test (impact speed and impact angle were set 70 km/h and 15°), as shown in the **Fig. 3.**

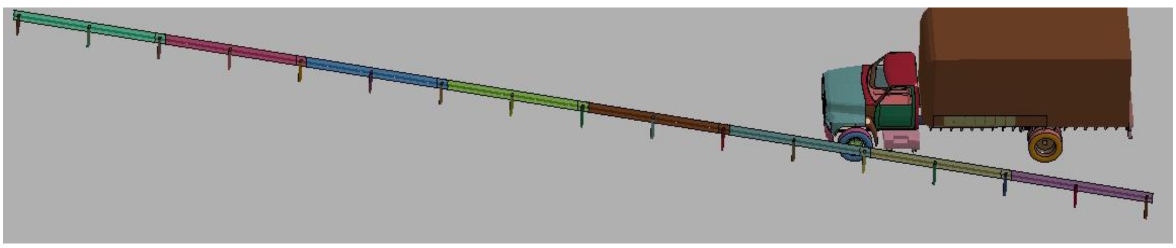

Figure 3. *Simulation model test*

The development and validation of a finite element model for W-beam guardrail according to European standard EN 1317 were proposed, details on the numerical model such as mesh parameters, soil modeled, boundary conditions, contact types, material model, etc. were explained in previous researches [33-36].

3. Impact testing model

Fig. 4 depicts the vehicle and W-beam guardrail models used in the impact test. The W-beam guardrails used in this study were ALKA AG04-2.0 guardrails [17]. The W-guardrail splice is 4,300 meters long. The C-post measures 1,600 mm in length and 950 mm in depth. The post dimensions are 125 mm x 62.5 mm x 25 mm. The truck selected from the NCAC database according to the European standard EN1317 [37].

Figure 4. *W-beam guardrail system and truck*

4. Boundary condition

W-beam guardrail continuation was represented by the addition of elastic springs at both ends of each node along the W-beam (**Fig. 5**). Post–soil interaction was represented using discrete spring elements attached to the posts. The stiffness of the nonlinear springs increased with depth and soil properties.

Roadway mode: was defined using RIGIDWALL_PLANAR card to simulate contact between the truck and the W-beam guardrail.

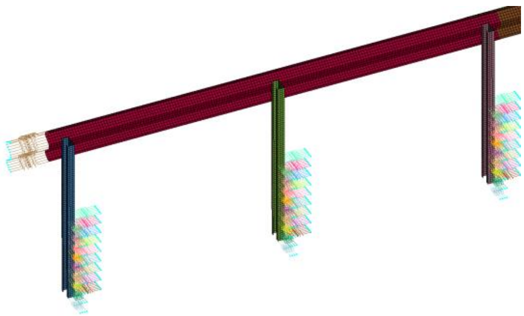

Figure 5. *Boundary condition*

IV. MODEL VALIDATION

Fig. 6 depicts a time sequence comparison between simulation results and the test outcomes. Experimental test was conducted by Ali Atahan et.al [17]. The crash test and simulation vehicles were effectively diverted. In TB 51 test, the experimental and simulated working widths were 1300 mm and 1280 mm, respectively. In TB 11 test, the validation model was introduced in detail in a previous study [36]. **Table 1** depicts a ASI and THIV comparison between experimental and simulation test.

Table 1. *Comparison between experimental and simulation [36]*

Evaluation Criteria	Experimental Result	Simulation Result
THIV (km/h)	31	26.1
ASI	0.94	0.93

There was an acceptable relationship between the test and simulation outcomes. Consequently, the model was validated and served as a baseline.

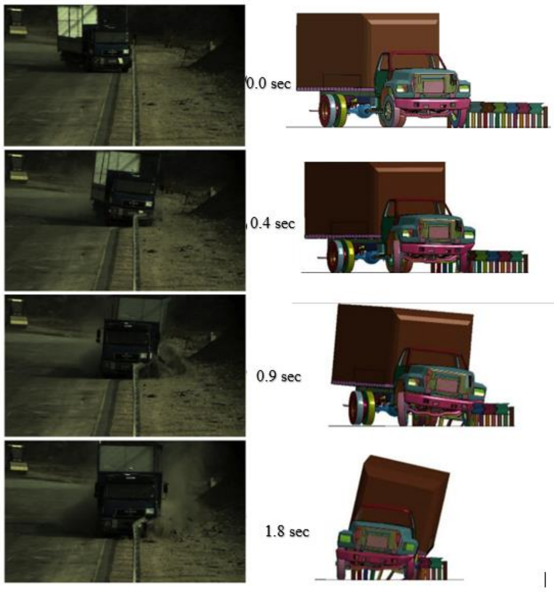

Experimental [9] Simulation

Figure 6. *Validation result on simulation*

V. RESULTS AND DISCUSSION

1. Effect of various post spacing and rail heights

The distances between the posts in the three models were 1333, 2000, and 4000 mm, respectively. All models had a W-beam guardrail height of 750 mm.

Fig. 7 shows the results of the TB42 impact test. These simulations illustrated that the W-beam guardrail prevented the vehicle from leaving the roadway.

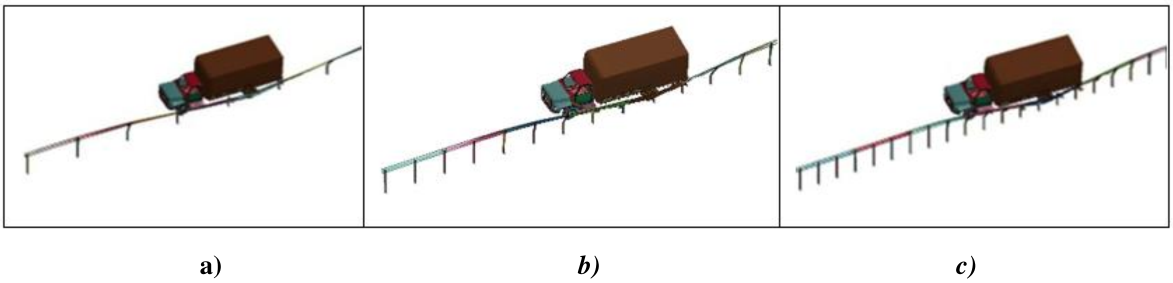

Figure 7. *Sequential of TB42 test with 4000 mm (a) 2000 mm(b) and 1333 mm (b) posts spacing*

The ASI, THIV, and the working widths of the impact tests are summarized in **Table 2**. These data show that the working width Wm of the guardrail post decreases proportionally to the distance between the posts. W-beam guardrails with post spacing 1333, 2000 and 4000 mm have working widths of 850, 1280 and 1450 mm, respectively. These values meet the working width classes of W3, W4 and W5. The W-beam guardrail meets the EN1317 standard in all three test conditions. W-beam guardrail with a distance between posts of 4000 mm have the highest ASI results (1.32), and to meet impact severity B. Both W-beam guardrails with a distance of 2000 mm and 1300 mm corresponding to impact severity A because the structure have ASI lower than 1. Compared to the other two post spacing, the W-beam guardrail with a post spacing of 2,000 mm gives the best protection under these test conditions. again.

Table 2. *Simulation TB42 test results with difference distance between posts*

Post spacing (mm)	THIV (km/h)	ASI	W_m (mm)
4,000	26.6	1.32	1450
2,000	24.6	0.87	1280
1,333	23.5	0.71	850

In simulations, the posts heights from the ground level were installed as follows: 800-, 750-, 700- and 650-mm. **Fig. 8** and **Table 3** represent the simulation results.

In all three cases, the W-beam guardrail can redirect the vehicle back to the roadway, which indicates that the W-beam guardrail meets EN 1317. There is a slight variation in the THIV value. Only the case of barriers up to a bar height of 650 mm has a working width class of W3, and the remaining have a working width class of W4. A W-beam guardrail height of 650 mm has the highest ASI value is 1.25 and a W-beam guardrail height of 800 mm represents the lowest ASI value is 0.72. The impact severity of 750 and 800 mm post height of W-beam guardrail corresponds to class A. The other collision W-beam guardrails correspond to class B. Therefore, 750 and 800 mm high W-beam guardrails carry a higher level of protection. The W-beam guardrail with a height of 800 mm and a spacing of 2,000 mm between posts has the lowest ASI, hence this structure provides better protection compared to the other.

Table 3. *Simulation TB42 test results with difference height of post*

W-beam guardrail height (mm)	THIV	ASI	Wm (mm)
650	26.6	1.25	980
700	26.5	1.1	1250
750	24.6	0.87	1280
800	24.3	0.72	1100

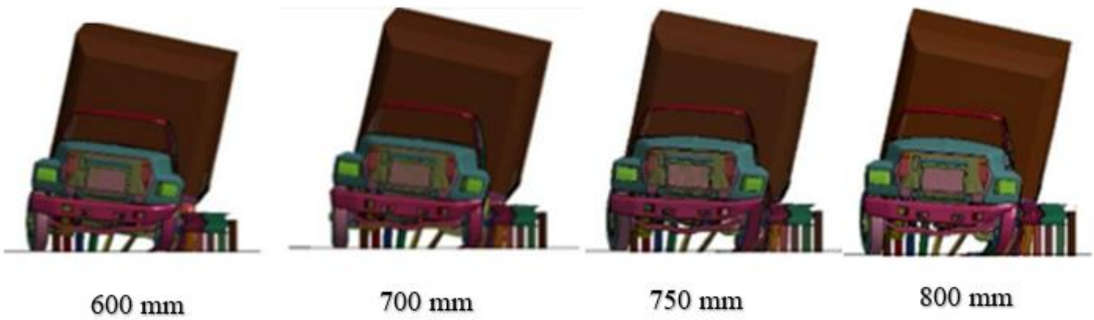

Figure 8. *Impact test results at different guardrail height*

2. Effect of soil properties

In this study, four various types of soil were used to simulate, various soil properties are described in the previous study [35-36].

Fig. 9-10 show the results of the road safety W-beam guardrail impact test. In all four conditions, the W-beam guardrail could prevent the vehicle from exiting the road and redirecting back into the lane.

In all four conditions, the W-beam guardrail meets the EN1317-2 standard for impact severity corresponding to class A. There is not much difference in ASI and THIV values, while there is a difference. very clear between working width values (**Table 4**). The results clearly confirm that soil properties do not affect the severity of impacts (ASI, THIV).

Table 4. *Simulation TB42 test results with various soil conditions*

Soil properties	THIV	ASI	Wm (mm)
Loose sand	24.6	0.87	1280
Medium sand	25.2	0.86	1350
Dense sand	26.8	0.86	1525
Very dense sand	25.7	0.88	1740

The results indicate that the W-beam guardrail's working width increases proportionally with the soil's abrasiveness. The results indicate that soil conditions have no effect on the impact severity (ASI, THIV) but do influence the deformation of the W-beam railing. The outcomes can be utilized as a guide for installing the W-beam guardrail system in different locations.

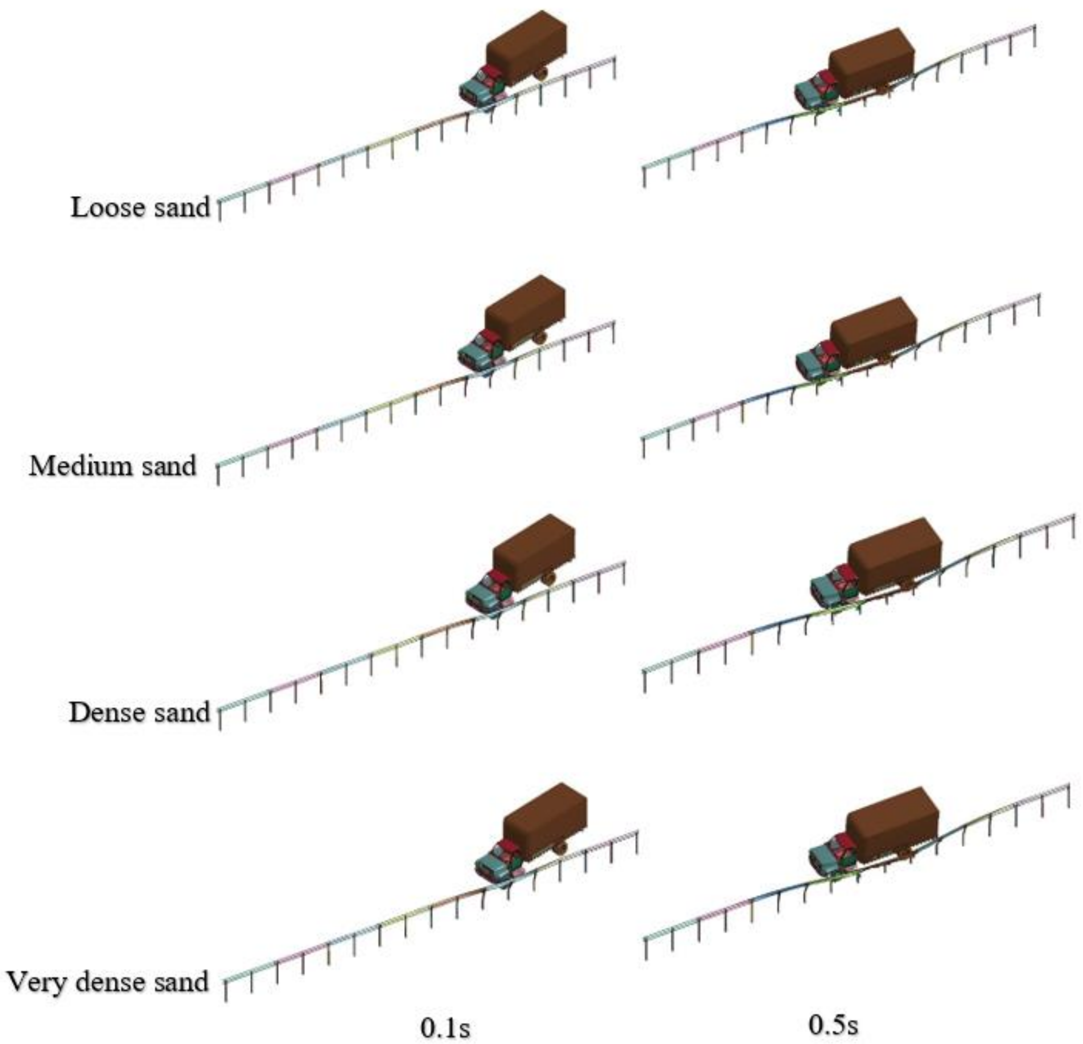

Figure 9. *Simulation TB42 test result with various soil properties*

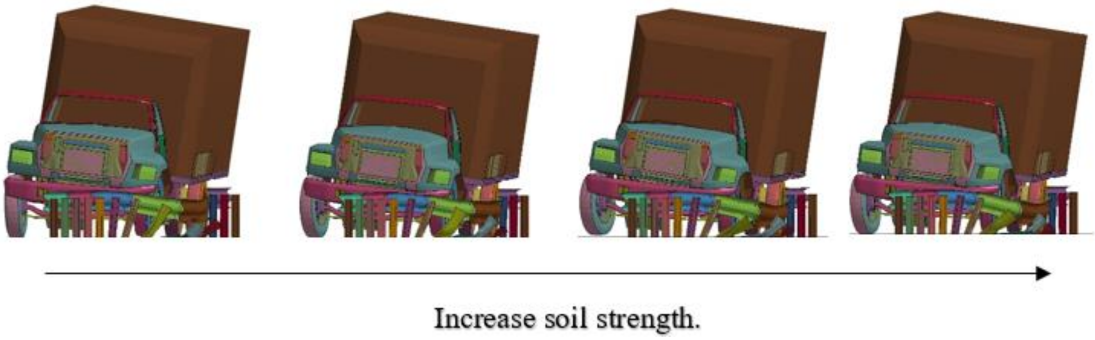

Figure 10. *W-beam guardrails with various soil conditions.*

3. Effect of different shaped post

The U-shaped, I-shaped, C-shaped, and Sigma-shaped post types have been analyzed and contrasted. The cross sections of the shaped posts are described in the previous research by Teng et.al [35].

Fig. 11-12 show simulation results when a truck impacts the guardrail at a speed of 70 km/h and a collision angle of 15 degrees. **Table 5** shows the severity of the impact (ASI and THIV) and the working width of the structures. All four cases, the guarail meets the EN1317-2 standard and has a W4 working width level. The W-beam I-beam guardrail provides a higher level of safety for vehicle drivers than in other cases. The I-shaped guardrail represents the biggest working width value is 1,340 mm and the W-shaped guardrail with C-shaped posts illustrates the lowest working width is 1,280mm.

Table 5. *Simulation test results with different shaped posts*

Soil properties	THIV	ASI	Wm (mm)
Loose sand	24.6	0.87	1280
Medium sand	25.2	0.86	1350
Dense sand	26.8	0.86	1525
Very dense sand	25.7	0.88	1740

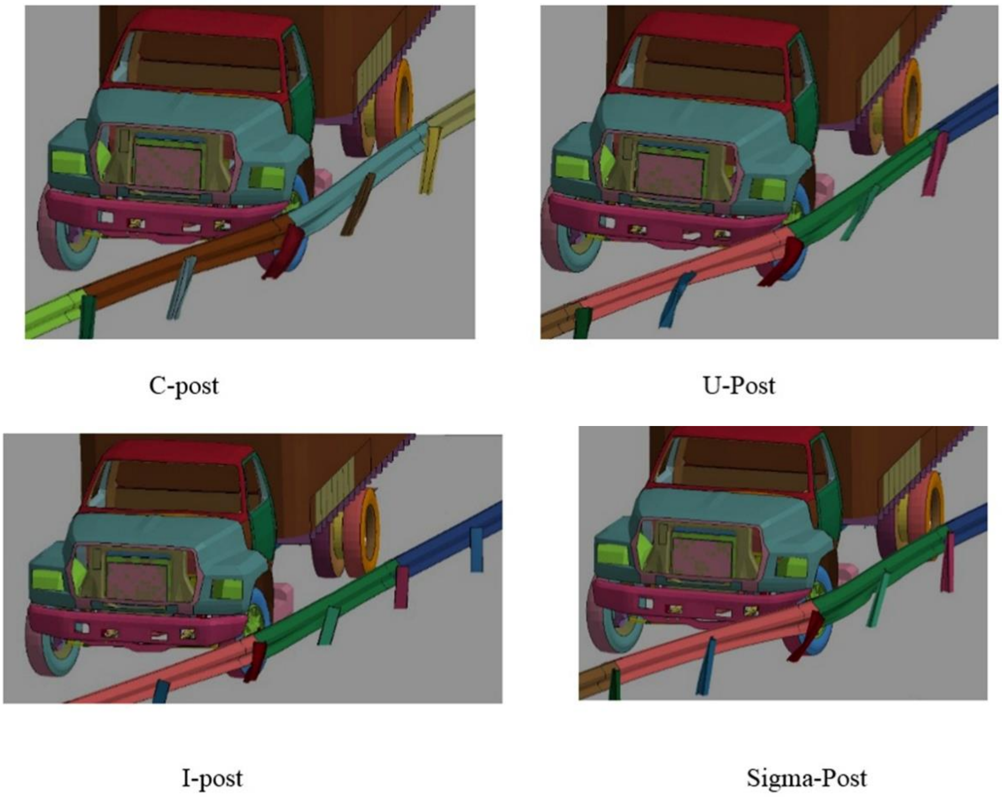

Figure 11. *Deformed of the W-beam guardrail system during TB42 impact test*

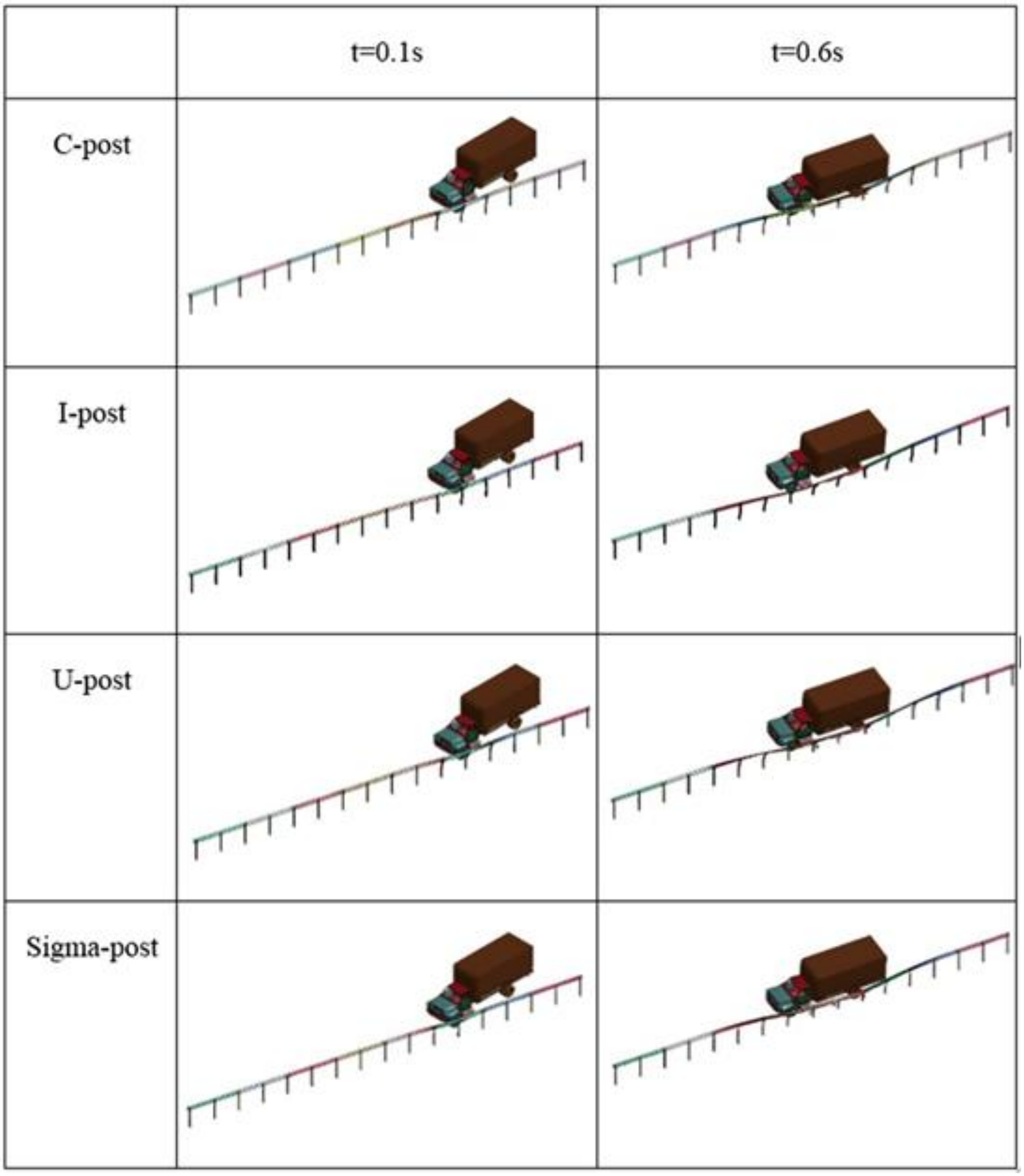

Figure 12. *Sequential figures from TB42 test with various shaped post*

VI. CONCLUSION

The study presents an investigation of the safety performance of the W-beam guardrail in various collisions according to the European standard EN1317 in collisions with a 10,000 kg truck. The study provides a very convenient way to increase the safety of W-guardrail guardrail. The main achievements, including contributions can be summarized as follows:

a) All W-beam guardrails with a 700 mm height and three-post spacing (4000, 2000 and 1333 mm) conform to the EN1317 standard. The working width of the W-beam guardrail decreases with the distance between the posts decreasing.
   – W-beam guardrail with span 1,333 and 2,000 mm corresponds to impact class A, and guardrail post W beam with span 4,000 mm has the highest ASI value and impact severity class B. Good level of protection The most in this case belongs to the W-beam guardrail with a distance between the posts of 1333 mm

b) For the four cases of height (650, 700, 750 and 800 mm) and the same post spacing of 2000 mm, the W-beam guardrail with a rail height of

800mm provides the highest level of protection.

c) Test simulations have been carried out demonstrating that different soil conditions do not affect the protection of the barrier according to the European standard EN1317. The results show that the properties of the soil do not affect the impact severity (ASI) but affect the working width. The working width of the W-beam guardrail increases in proportion to the stiffness of the soil.

d) For various shaped post
   – The best protection is in the W-beam guardrail with the cross-section of the I-shaped post. The worst protection is in the W-beam guardrail with the Sigma cross-section.

AUTHOR CONTRIBUTIONS

Tran Thanh Tung: Conceptualization, Finite element modelling, Writing,

Tso-Liang Teng: Review and editing.

DISCLOSURE STATEMENT

The authors declare that they have no known competing financial interests or personal relationships that could have appeared to influence the work reported in this paper.

REFERENCES

[1] The Institution of Engineering and Technology: Glossary of Safety Terminology. No.00, 2017. https://www.theiet.org/impact-society/factfiles/engineering-safety-factfiles/glossary-of-safety-terminology/

[2] United States Department of Transportation, Insurance Institute of Highway Safety (IIHS). Collisions with fixed objects and animals, 2021. https://www.iihs.org/topics/fatality-statistics/detail/collisions-with-fixed-objects-and-animals

[3] Wang, J.; Lu, H.; Sun, Z.; Wang, T.; Wang, K. Investigating the Impact of Various Risk Factors on Victims of Traffic Accidents. Sustainability, 12 (9) (2020) 3934. https://doi.org/10.3390/su12093934

[4] Molan, A.M.; Rezapour, M.; Ksaibati, K. Investigating the relationship between crash severity, traffic barrier type, and vehicle type in crashes involving traffic barrier. Journal of Traffic and Transportation Engineering 7 (1) (2020) pp. 125–136. https://doi.org/10.1016/j.jtte.2019.03.004

[5] International Transport Forum. Road Safety annual report 2021. https://www.itf-oecd.org/road-safety-annual-report-2021 (accessed May 2023)

[6] Type of Crash https://injuryfacts.nsc.org/motor-vehicle/overview/type-of-crash/ (accessed May 2021)

[7] Federal Highway Administration. https://safety.fhwa.dot.gov/roadway_dept/ (accessed May 2021)

[8] Trinity Highway. https://trinityhighway.com/product/t-31-guardrail/ (accessed May 2021)

[9] The National Road Safety Strategy. National Road Safety Action Plan 2023-5. https://www.roadsafety.gov.au/action-plan/national-road-safety-action-plan-2023-25

[10] Albuquerque F.D.B., Awadalla DM. Roadside fixed-object collisions, barrier performance, and fatal injuries in single-vehicle, run-off-road crashes. Safety, 6 (2) (2020), p. 27. https://doi.org/10.3390/safety6020027

[11] Safe German Guardrail Technology. Heintzmann Basic W-beam guardrail. http://www.heintzmann.eu

[12] Qiao, W.; Huang, E.; Guo, H.; Liu, Y.; Ma, X. Barriers Involved in the Safety Management Systems: A Systematic Review of Literature. International Journal of Environmentral Research and Public Health, 19 (15) (2022) 9512. https://doi.org/10.3390/ijerph19159512

[13] W beam 4mm thickness base metal crash barrier guardrail, Shandong Huaan Traffic Facilities Co., Ltd. https://www.guardrailfactory.com/gb-guardrails/w-beam-4mm-base-metal-crash-barrier-guardrails.html

[14] Crash Barrier Systems Market Report 2022 – Market Forecast, Trends And Strategies, 2022. https://www.thebusinessresearchcompany.com/press-release/crash-barrier-systems-market-2022

[15] European Standard EN 1317–1, EN 1317–2:2010. Road restraint systems.

[16] AASHTO. Manual for Assessing Safety Hardware (MASH). Washington, DC: American Association of State Highway and Transportation Officials (AASHTO), 2009.

[17] Atahan AO, Yucel AO, Erdem MM. Crash testing and evaluation of a new generation L1 containment level guardrail. Engineering Failure Analysis 38 (2014) pp. 25-37. https://doi.org/10.1016/j.engfailanal.2014.01.003

[18] Matthew Gutowski, Emre Palta, Howie Fang. Design optimization of a new W-beam

guardrail for enhanced highway safety performance. Advances in Engineering Software, 112 (2017) pp. 154-164. https://doi.org/10.1016/j.advengsoft.2017.05.002

[19] Matej Borovinšek, Matej Vesenjak, Zoran Ren. Improving the crashworthiness of reinforced wooden road safety W-beam guardrail using simulations of pre-stressed bolt connections with failure. Engineering Failure Analysis 35 (2013) pp. 625-635. https://doi.org/10.1016/j.engfailanal.2013.06.006

[20] Mehrtash Soltani, Taher Baghaee Moghaddam, Mohamed Rehan Karim, N.H. Ramli Sulong. Analysis of developed transition road safety barrier systems. Accident Analysis and Prevention, 59 (2013) pp. 240-252. https://doi.org/10.1016/j.aap.2013.05.029

[21] Amirarsalan Mehrara Molan , Khaled Ksaibati. Impact of side traffic W-beam guardrail features on the severity of run-off-road crashes involving horizontal curves on non-interstate roads. International Journal of Transportation Science and Technology, 10 (3) (2021) pp. 245-253. https://doi.org/10.1016/j.ijtst.2020.07.006

[22] Plaxico CA, Guardrail MH and Hiranmayee K. Compariosn of the impact performance of the G4 (1S) and G4 (2S) guardrail systems under NCHRP report 350 Test 3-11 conditions

[23] M I Gheres and I L Scurtu. Crash testing and evaluation of W-beam guardrail using finite elements method. IOP Conference Series: Materials Science and Engineering, 1220 (2021) 012049. http://doi.org/10.1088/1757-899X/1220/1/012049

[24] Ferduos MR, Odeh AA, Bligh RP, et al. Performance limit analysis for common roadside and median W-beam guardrail using LS-DYNA. International Journal of Crashworthiness, 16 (6) (2011) pp. 691-706. https://doi.org/10.1080/13588265.2011.623023

[25] Lee DW, Ahn JS, and Woo KS. Vehicle impact analysis of flexible W-beam guardrail supported by different shaped posts in sloping ground. Advances in Mechanical Engineering, 6 (2014). https://doi.org/10.1155/2014/705629

[26] W-Beam Guardrail, Materials Handling Pty Ltd. https://www.materialshandling.com.au/products/w-beam-guardrail/

[27] Flexbeam Guardrail Crash W-beam guardrail https://www.ingalcivil.com.au/products/road-safety-barriers/guardrail/flexbeam

[28] W-Beam Guardrail Effectively Makes the Highway Safer https://www.highway-guardrail.com/highway/w-beam-guardrail.html

[29] Safe Direction. Protecting Life& Property. W-beam guardrail semi-rigid protection. Product manual. Ref: PM 003/01. http://www.safedirection.com.au

[30] NZ Transport Agency. Specification and guidelines for road safety hardware and devices. NZTA M23A: 2022. https://www.nzta.govt.nz/assets/resources/road-safety-barrier-systems/docs/m23-road-safety-barrier-systems.pdf

[31] Voestalpine. Vehicle restraint system. http://www.voestalpine.com/strassensicherheit/en/products

[32] Fracasso hellas- Quality in Safety. http://www.fracassohellas.gr

[33] Tso-Liang Teng, Cho-Chung Liang, Thanh-Tung Tran, Effect of various W-beam guardrail post spacings and rail heights on safety performance, Advances in Mechanical Engineering, 7 (11) (2015) p. 16. https://doi.org/10.1177/1687814015615544

[34] Tso-Liang Teng, Cho-Chung Liang, Ching-Yu Hsu, Chien-Jong Shih, Thanh-Tung Tran, Impact Performance of W-beam Guardrail Supported by Different Shaped Posts, International Journal of Mechanical Engineering and Applications, 4 (2) (2016) pp. 59-64. https://doi.org/10.11648/j.ijmea.20160402.14

[35] Tso-Liang Teng, Cho-Chung Liang, Ching-Yu Hsu, Chien-Jong Shih, Thanh-Tung Tran. Effect of Soil Properties on Safety Performance of W-beam Guardrail. Proceedings of the 2016 International Conference on Advanced Materials Science and Environmental Engineering. https://doi.org/10.2991/amsee-16.2016.10

[36] Teng T-L, Liang C-C, Tran T-T. Development and validation of a finite element model for road safety W-beam guardrail impact tests. Simulation, 92 (6) (2016) pp. 565-578. https://doi.org/10.1177/0037549716644507

[37] NHTSA Crash Simulation Vehicle Models https://www.nhtsa.gov/crash-simulation-vehicle-models

ACTA TECHNICA JAURINENSIS
Vol. 16, No. 3, pp. 116-122, 2023
10.14513/actatechjaur.00705

Alternative Routes for Deliveries of Kazakh Crude Oil Shipments to the European Union

Erjan Akhmedov [1,*]

[1]Business School, Kazakh-British Technical University, Tole Bi St. 59, Almaty, 050000, Kazakhstan
*e-mail: e.akhmedov@kbtu.kz

Submitted: 19/06/2023 Accepted: 26/06/2023 Published online: 07/07/2023

Abstract: The situation with crude oil shipments from Kazakhstan to the European Union has seriously deteriorated since 24 February 2022 when Russia started its invasion of Ukraine. A series of different incidents, which complicated these deliveries, started soon after the beginning of the invasion and this has again brought to light the need to diversify the export routes for the Kazakh crude oil. In spite of numerous previous appeals, the dependence on the transit via the Russian territory only increased over the last years. This paper analyses the reasons for this increased dependence, considers the alternative routes and their attending circumstances and attempts to suggest potential ways out of this situation. Considering this topic, it is essential to mention that Kazakhstan is among the five top suppliers of crude oil to the European Union, and, at the same time, the European Union is the biggest importer of Kazakh crude oil.

Keywords: European Union; Kazakhstan; crude oil; export routes; export routes diversification; Russo-Ukrainian war

I. INTRODUCTION

First of all, the author would like to provide evidence of how mutually dependent in terms of crude oil trade the European Union (EU) and Kazakhstan are.

Though information on EU imports of crude oil may look a bit outdated, the situation has not changed much within the last few years and this is shown on **Fig. 1** and **Fig. 2**. In spite of some variations, the share of Kazakhstan remains substantial and the country continues to be among the top exporters of crude oil to the European Union.

However, since 24 February 2022 the overall context started to change. Already, in August 2022 it was stated in [1] that “Kazakhstan is dependent on Russia for its main oil export route, which has run into repeated problems since Nur-Sultan (the capital of Kazakhstan) refused to support Moscow’s war.”

Keeping all the political reasonings aside, it is important for any exporter to diversify its export routes as it allows to build resilience to unexpected developments. It is equally important for an importer to ensure safe, reliable and uninterrupted supplies of energy.

The key oil export routes for the Kazakh crude are shown in **Fig. 3**.

CPC – Caspian pipeline consortium pipeline, BTC – Baku-Tbilisi-Ceyhan pipeline

This article is attempting to answer the following research questions:

1) What are the reasons for overdependence of Kazakhstan for its crude oil exports via the Russian territory? and
2) How to get rid of this dependence?

II. LITERATURE REVIEW

Starting this section, the author needs to admit that the topic of this article is not in the limelight of researchers. This becomes especially evident in comparison with shipments from the Middle East. Nonetheless, the author has attempted to analyse as many literature sources as possible. Information collected by the author at various oil and transportation conferences and other professional events over the past few years is also used widely.

“A brief overview of the political economy of Caspian oil” is provided in [2]. The same source raises “the critical problem – ... reliance on evacuation routes that run through Russia.

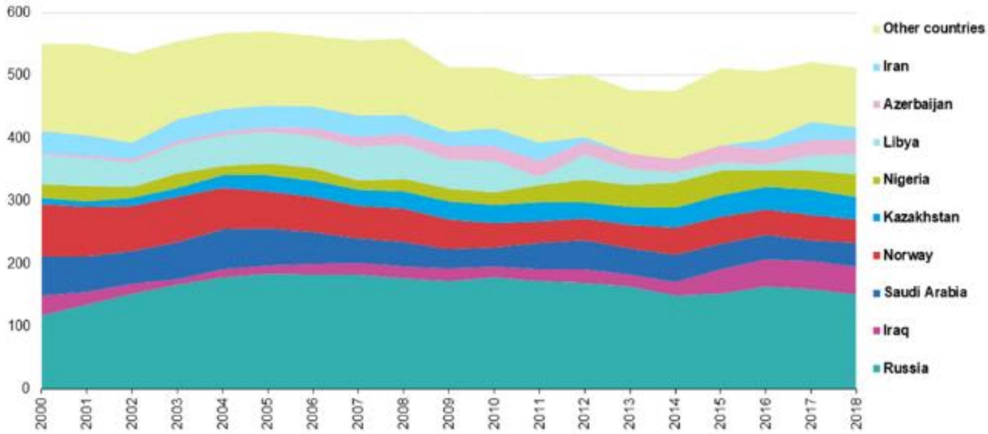

Figure 1. *Crude oil imports by country of origin, EU-27, 2000-2018 (million tonnes) [3].*

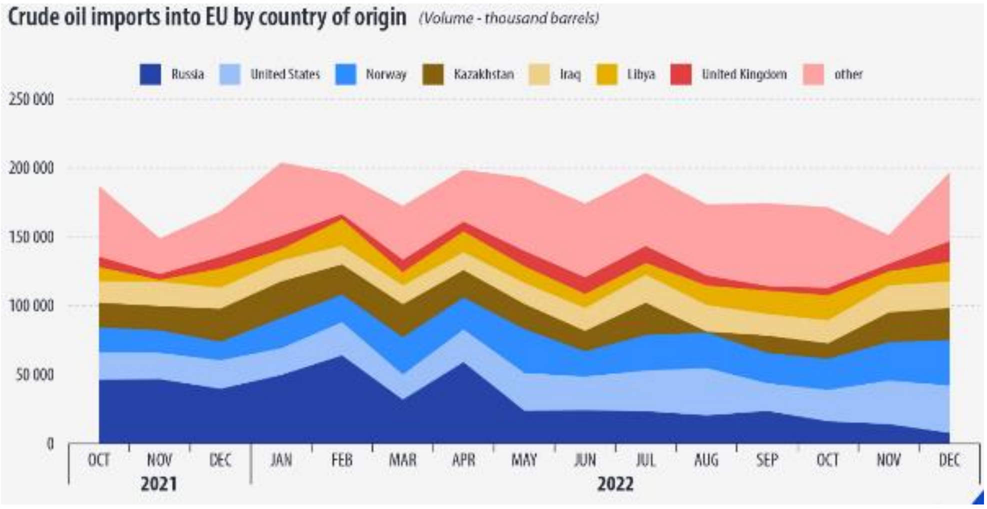

Figure 2. *Crude oil imports into EU by country of origin (volume – thousand barrels) [4].*

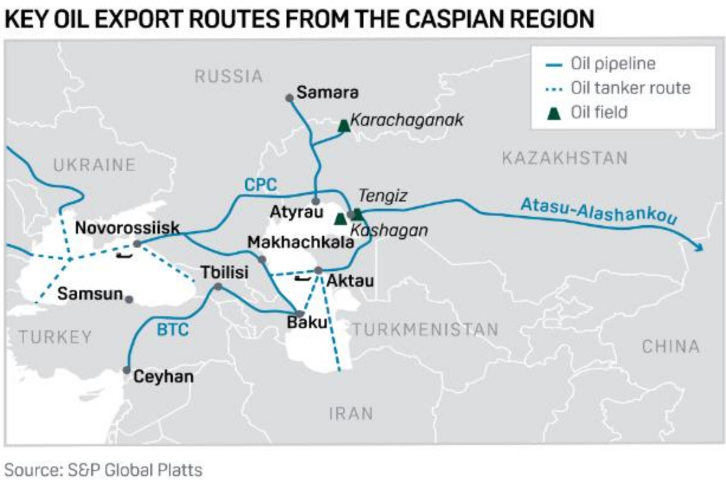

Figure 3. *Key Oil Export Routes from the Caspian Region [5].*

Diversification of export routes was recognised as an important goal after 1991 but was impeded by the geopolitical difficulties presented by many of the possible alternatives." In their another manuscript [6], the same authors admitted that "Kazakhstan's desire to diversify export routes and reduce its dependence on Russia notwithstanding, evacuation routes via the Russian Federation remain in some cases the least problematic, given the difficulties posed by disputes over the Caspian and by political factors in Iran and Turkmenistan." The issue of export routes diversification was further developed in [7]: "Kazakhstan is keen to improve exporting capacities and is looking for options to diversify export routes."

The energy cooperation between the EU and Kazakhstan (and other Caspian region countries) was addressed in [8]. It this source Kazakhstan is mentioned as the EU's "most important oil partner in CACR (Central Asia and the Caspian Region)". In [9] it is analysed "how the security of oil supply to the European Union member states could be enhanced in case of a lasting supply disruption…" In [10] the authors assessed energy security in the Caspian Region and its geopolitical implications for the European energy strategy. In [11] it is mentioned that "West European countries perceive increasing their supplies from the Caspian region as a way to lessen their dependence on oil coming from OPEC-associated countries, especially the Persian Gulf." Other publications which addressed this topic include [12] and [13]. The paper [12] assessed the role of the Black Sea region (which is geographically very close to the Caspian region) in the European energy security making some important observations like "The EU has acknowledged the great oil and natural gas potential of the Caspian Sea region. The oil and natural gas resources of the states of the Caspian Sea littoral could provide a temporary alternative energy supply if Russia interrupts again the oil exports" and "An integral part of an increased focus on Caspian hydrocarbons must be concerted EU action against Russian threats to the east-west corridor". The same topic of the European Union Energy Security was continued in [13]. The authors reiterate that "Diversification of energy resources is one of the objectives for the EU" and analyse "the potential of the Caspian basin in terms of energy and its impact on the energy security of the European Union".

A major part of publications related to the topic of this manuscript is in Russian language. It is reasonable to mention such works as [14], [15], [16], [17], [18] and [19]. [14] provides a detailed overview of different transportation routes for the Caspian oil and gas. Continuing this topic, the authors of [15] study various factors (physical-geographical, technological, economic, political, environmental) that influence the choice of optimal transportation options for the Caspian Sea hydrocarbons. They also propose a mathematical model, which takes into consideration the mentioned factors and suggests an optimal transportation option. In [16] prospects for offshore oil and gas production in the Northern Caspian Sea and possible ways of transportation are being investigated. In [17] economic and regional factors of the development of hydrocarbon transportation systems in Russia including the Caspian Sea region are addressed. The author of [18] investigates special aspects of the development of oil and petroleum products transportation by different modes of transport. [19] deserves special mentioning. In this work transportation flows and routes and competition between different modes of transport are considered.

Several publications considered the development of transport infrastructure of Kazakhstan and the neighbouring countries. They include [20], [21] and [22]. Considering challenges and prospects of the Kazakh infrastructure development, the authors of [20] pay special attention to the accessibility of global communication routes for Kazakhstani exports. In contrast, the paper [21] analyses the transport infrastructure of Russia's oil and gas industry "as regards the location of economic activity and existing transport links in that sphere, competitiveness of various modes of transport in transporting oil and gas cargoes, existing problems and approaches to solving them." And in the [22], "the potential demand for oil and oil products transport via the existing rail corridor in the Caucasus, taking into consideration the competition from alternative routes" is evaluated.

Another important source of information became the publications of international organizations like [23], [24] and [25] and professional associations [26]. Here it is essential to acknowledge that these sources of information usually provide accurate information quite quickly. Even if this information is not used directly, it provides abundant material for further thought or for understanding the context.

III. DATA AND METHODOLOGY

Data collection for this article was based on the following:

1) Review of different literature sources. As already mentioned in the Literature review section above, the body of relevant literature is quite limited.
2) Gathering information at oil and gas conferences and other professional events. Over the last several years, the author attended and spoke (both on- and off-line) at numerous events in Azerbaijan, Hungary, Kazakhstan, the Netherlands, and Russia.
3) Gathering information from market players and representatives of academia. These sources are invaluable for understanding the situation.

The criteria for including studies into consideration were their relevance to the topic, reliability and objectivity. The same principles were applied while gathering information at professional events and from market players and academia representatives, adding to them the trustworthiness of market players, speakers at and participants of professional events.

In order to minimise the risk of bias, the information gathered at professional events and from market players was cross-checked. Clarification calls were made when necessary.

The analytical part of this paper was initially discussed with market players and academia representatives and then presented at two oil and gas conferences. Comments and recommendations received helped to improve the quality of this research. The market players and academia representatives whom the author discussed the content of this article with agreed that the selected methodological approach is suitable for the research questions mentioned above.

List of interviewees

The following oil and gas and transportation professionals and representatives of academia agreed to share their views on the situation:

1) Vice-president for operations, Kazakh oil transportation company;
2) Business development manager, multinational oil company operating in Kazakhstan;
3) Director of export department, mid-size Kazakh oil company;
4) Manager, oil market intelligence agency;
5) Transport manager, Kazakh oil company;
6) Representative of the Ministry of Energy of Kazakhstan;
7) Professor, Kazakh research institution specialized in transport subject area;
8) Associate professor, Kazakh university
9) Associate professor, Azerbaijan university

IV. Results and Discussion

The distinctive aspect of the considered problem is the dependence of Kazakh oil producer on export routes transiting the Russian territory (CPC and Atyrau-Samara pipelines) has substantially increased over the last years from 64% in 2010 to 95% in 2021 (**Table 1**-**2**).

All percentages do not total 100% due to rounding. Let us have a look at the reasons for this increase.

Table 3 above clearly demonstrates that the economics of crude oil export via CPC pipeline is much better in comparison with other routes. It is also the shortest route, which results in shorter delivery times and better safety. The CPC pipeline is also safer from the environmental point of view as it has less trans-shipments and requires less time for transportation. It also has the quality bank. This circumstance is of serious importance for producers of high quality crudes. Last, but not least is the fact that major Kazakh oil producers have shares in CPC. All these reasons made CPC the major export route for the Kazakh crude. The only what complicates further shipments via CPC is the changed political situation. This changed situation can lead to even discontinuation of shipments via the Russian territory.

Table 1. *Export of crude oil from Kazakhstan, 2010 [27].*

	Route	Amount, mln. metric tons	Share, %
1.	Caspian pipeline consortium pipeline (CPC)	29.9	42
2.	Atyrau-Samara pipeline	15.3	22
3.	Port of Aktau	9.3	13
4.	Atasu-Alashankou pipeline (to China)	10.1	14
5.	Railway	6	8
6.	Total	70.6	

Table 2. *Export of crude oil from Kazakhstan, 2021 [27].*

	Route	Amount, mln. metric tons	Share, %
1.	Caspian pipeline consortium pipeline (CPC)	53	78
2.	Atyrau-Samara pipeline	12	17
3.	Port of Aktau	2	3
4.	Atasu-Alashankou pipeline (to China)	1	1
5.	Railway	insignificant amounts	
6.	Total	68	

Table 3. *Economics of crude oil export from Kazakhstan, 2021 [27].*

	Route	Tariff, $ / ton
1.	Caspian pipeline consortium pipeline (CPC)	38
2.	Atyrau-Samara-Vysotsk (Russian Baltic Sea port)	56
3.	Port of Aktau – port of Baku and then via BTC pipeline	113
4.	Atasu-Alashankou pipeline (to China)	45
5.	Railway from Atyrau to Batumi (Georgian Black Sea port)	103

A substantial portion of crude oil produced in Kazakhstan has been transported via the Atyrau-Samara pipeline and then via the Russian Transneft crude oil pipeline system. Unfortunately, this route is becoming risky because of tightening anti-Russian sanctions. The shipments of the Russian crude via the Transneft system were almost discontinued. It is unlikely that revenues from relatively small Kazakh shipments will be enough to support the functioning of this system in the future.

At first glance, the economics of shipments to China also looks attractive. However, this is the tariff till the border between China and Kazakhstan only. It is important to note here that the main consumers of crude oil and refined products in China are in the eastern coastal provinces. So, if we take into consideration the distance between the point where the Atasu-Alashankou pipeline crosses the border between China and Kazakhstan and say the city of Shanghai, the actual tariff for Chinese consumers should be more than doubled.

In the event the shipments of Kazakh crude via the Russian territory are discontinued, increasing refining or using crude oil in petrochemistry can be a partial solution. Within the last few years, the share of the total production, which was used for these purposes was around 20%. However, the share of these industries should be significantly increased due to their rapid development over the last several years.

The route via the port of Aktau, then by sea to the port of Baku and finally to the Mediterranean via the BTC (Baku-Tbilisi-Ceyhan) pipeline is the most expensive option. There are also issues around the access to this pipeline, which do not exist for CPC. In spite of the high cost, this route can become a partial solution. Similarly, railing the Kazakh crude oil from Atyrau to Batumi (Georgian Black Sea port) via the territory of Azerbaijan is very expensive. In addition to that, this route crosses the Russian territory.

Meanwhile, there is a need to look at other potential export routes, which have not been covered above. The first is supplying the North of Iran via Turkmenistan by rail or via the Caspian Sea to Iranian sea ports by sea (please refer to the map on **Fig. 3** above). This option existed in the past and was discontnued because of Western sanctions against this country (Iran). Another potential destination is the neighboring countries: Afghanistan, Kyrgyzstan and Uzbekistan. However, the demand in these countries is relatively small – never exceeded 1 million metric tons.

V. CONCLUSIONS AND RECOMMENDATIONS

1) CPC remains to be the best export route for the Kazakh crude at the moment and in the near future. However, this does not mean that the situation can be accepted as is. The work on the development of alternative routes has to be continued even if alternatives are less attractive economically now. There is a possibility that all transit via Russia (or at least via the Russian Black Sea ports) will be discontinued due to political or security reasons. In this case, even more expensive and difficult routes bypassing the Russian territory will be needed for the country.
2) Among the most viable alternatives to CPC are shipments to the port of Aktau and then to the Mediterranean via BTC pipeline and to China via the Atasu-Alashankou pipeline, though substantial investments are required to make them able to accept increased volumes. In spite of these investments, high transportation costs and other issues, these two routes remain the only feasible options for the evacuation of the Kazakh crude to the World markets in sizeable quantities.
3) Construction of the Caspian undersea pipeline from Aktau to Baku (please refer to **Fig. 3** above) can radically decrease the cost of transportation via this route. However, this project is very costly and involves numerous environmental problems.
4) The routes via Turkmenistan to Iran or from the port of Aktau via the Caspian Sea to Iranian sea ports are not operational now due to the Western sanctions. In the event these sanctions are lifted, these routes will soon become very attractive.
5) Another potential way is to increase crude oil refining or using crude oil in petrochemistry. This way is also not free from limitations and requires additional investments but can at least partially ease the situation.
6) In spite of limited demand in the neighbouring countries of Afghanistan, Kyrgyzstan and Uzbekistan, the shipments to these countries deserve due attention. It should be noted that though the demand in these countries is quite small it has a steady upward trend because of rapidly growing populations.
7) The Turkmenistan–Afghanistan–Pakistan–India (TAPI) gas pipeline project is being considered. In case this project moves forward, an oil pipeline can be laid down in parallel with this gas pipeline's right-of-way (in compliance with all the required technical safety standards).
8) In spite of tightening anti-Russian sanctions, potential swap deals with Russia can be a partial solution as well. In this case, Kazakh oil producers can supply crude oil to China via the Atasu-Alashankou pipeline and receive equivalent volumes of Russian crude in say Russian Baltic Sea ports.
9) The country has to continue clarifying to the international community that shipments from Kazakhstan are not subject to sanctions. This is critical as there were attempts to restrict Kazakh cargoes already.

Research contribution

The present study is among the first and very few, which considers the changed situation with energy supply to the European Union since the beginning of the Russo-Ukrainian way. As mentioned above, the literature body on this topic is limited, though the importance of crude oil supplies from Kazakhstan to the EU is high.

Research limitations

1) Small sample size: the limitation is caused by the nature of the research. Here it is necessary to acknowledge that the overall number of people with proper understanding of the situation and the market trends is limited. The author, however, tried his best to increase the number of respondents as much as possible.
2) Self-reported data: the limitation is also caused by the nature of my research. It was addressed through cross-checking the answers, making clarification calls to ascertain the responses and comparing the information received from the respondents with the information presented in different publications (mainly of international organizations and professional associations).
3) Refusal to comment on some issues due to political and/or self-censoring reasons. This situation is very typical for the oil and gas industry.

The limitations above do not undermine the value of this, but rather serve as an initial point of departure for further studies.

AUTHOR CONTRIBUTIONS

E. Akhmedov: Conceptualization, Experiments, Theoretical analysis, Writing, Review and editing.

DISCLOSURE STATEMENT

The authors declare that they have no known competing financial interests or personal relationships that could have appeared to influence the work reported in this paper.

ORCID

Erjan Akhmedov https://orcid.org/0000-0002-7869-6920

REFERENCES

[1] Kumenov Almaz, "Kazakh oil exports across Russia interrupted for fourth time this year," Aug. 23, 2022. https://eurasianet.org/kazakh-oil-exports-across-russia-interrupted-for-fourth-time-this-year

[2] R. Ahrend and W. Tompson, "Caspian oil in a global context," *Transition Studies Review*, vol. 14, no. 1, pp. 163–187, May 2007, https://doi.org/10.1007/s11300-007-0132-5

[3] Crude oil imports by country of origin, EU-27, 2000-2018. Eurostat, 2 July 2020. https://ec.europa.eu/eurostat/statistics-explained/index.php?title=File:Crude_oil_imports_by_country_of_origin,_EU-27,_2000-2018_(million_tonnes)_F.png

[4] Crude oil imports and prices: changes in 2022, Eurostat, 28 March 2022. https://ec.europa.eu/eurostat/en/web/products-eurostat-news/w/DDN-20230328-1

[5] Kazakhstan's Tengiz oil field operator says logistics problem impacting output amid political crisis, S&P Global Commodity Insights, 7 January 2022. https://www.spglobal.com/commodityinsights/en/market-insights/latest-news/oil/010622-kazakhstans-tengiz-oil-field-operator-says-logistics-problem-impacting-output-amid-political-crisis

[6] R. Ahrend and W. Tompson, "Realising the Oil Supply Potential of the CIS: The Impact of Institutions and Policies," Elsevier BV, Dec. 2007. https://doi.org/10.2139/ssrn.1010667

[7] F. Guliyev and N. Akhrarkhodjaeva, "The Trans-Caspian energy route: Cronyism, competition and cooperation in Kazakh oil export," *Energy Policy*, vol. 37, no. 8, pp. 3171–3182, Aug. 2009, https://doi.org/10.1016/j.enpol.2009.04.009

[8] F. Umbach and S. Raszewski, "Strategic Perspectives for Bilateral Energy Cooperation between the EU and Kazakhstan - Geo-economic and Geopolitical Dimensions in Competition with Russia and China's Central Asia Policies," Berlin, 2016. www.eucers.eu

[9] Kottsieper, "Study on the Technical Aspects of Variable Use of Oil Pipelines-Coming into the EU from Third Countries OVERALL REPORT Prepared for the Directorate-General for Energy of the European Commission," Munich, 2010. https://ec.europa.eu/energy/sites/ener/files/documents/2010_reporting_technical_aspects.pdf

[10] U. Aydin and D. Azhgaliyeva, "Assessing Energy Security in The Caspian Region: The Geopolitical Implications for European Energy Strategy," Tokyo, 2019. https://www.adb.org/publications/assessing-energy-security-caspian-region

[11] J. Cichocki, "The Significance of Caspian Oil and Gas for Diversifying Energy Imports to the Visegrad Group Countries," *Connections*, vol. 2, no. 1, pp. 23–28, 2003. https://www.jstor.org/stable/26322975?seq=1#metadata_info_tab_contents

[12] C. Lupu, "The Russia and EU at crossroads. The role of the Black Sea region in the European energy security," Università degli Studi di Trieste, Trieste, 2009. https://core.ac.uk/download/pdf/41172151.pdf

[13] A. Ibrayeva, D. V. Sannikov, M. A. Kadyrov, V. N. Zapevalov, E. L. Hasanov, and V. N. Zuev, "Importance of the Caspian Countries for the European Union Energy Security," *International Journal of Energy Economics and Policy*, vol. 8, no. 3, pp. 150–159, 2018. http://www.econjournals.com/index.php/ijeep/article/view/6263

[14] S. Makarova, "Export routes and transportation of Caspian oil and gas," *Social and economic geography*, 2005. https://cyberleninka.ru/article/n/2005-03-011-014-eksportnye-marshruty-i-transportirovka-kaspiyskoy-nefti-i-gaza

[15] M. Petrov and V. Lubenko, "Factors Influencing the Choice of Optimal Caspian Sea Shelf Hydrocarbon's Transportation," *Bulletin of the Astrakhan State Technical University*, 2009. https://cyberleninka.ru/article/n/faktory-opredelyayuschie-optimalnuyu-shemu-transportirovki-uglevodorodov-shelfa-kaspiyskogo-morya

[16] M. Petrov and V. Lubenko, "The Forecast of the Marine Oil and Gas Development and the Possible Method of Oil Transportation on the Shelf of the North Caspian Sea," *Bulletin of the Astrakhan State Technical University*, 2008. https://cyberleninka.ru/article/n/perspektivy-morskoy-dobychi-nefti-i-gaza-na-shelfe-severnogo-kaspiya-i-vozmozhnye-sposoby-ih-transportirovki

[17] E. Markushina, "Economic and regional factors in the development of hydrocarbon transportation systems," *Scientific and technical statements of St. Petersburg State Polytechnic University. Economics*, 2011. https://cyberleninka.ru/article/n/ekonomicheskie-i-regionalnye-faktory-razvitiya-sistem-transportirovki-uglevodorodov

[18] A. Smirnova, "Features of the development of transportation of oil and oil products by various modes of transport," *Bulletin of Kazan Technological University*, 2012. https://cyberleninka.ru/article/n/osobennosti-razvitiya-perevozki-nefti-i-nefteproduktov-razlichnymi-vidami-transporta

[19] Yu. A. Shcherbanin, "Export Deliveries of Oil and Petroleum Products: Flows, Routs, Transport Mode's Competition," *Design, Construction and Operation of Gas and Oil Pipelines and Storages*, vol. 1, pp. 22-27`, 2017. https://cyberleninka.ru/article/n/postavka-nefti-i-nefteproduktov-na-eksport-potoki-napravleniya-konkurentsiya-vidov-transporta/viewer

[20] Z. B. Akhmetova, Zh. T. Kozhamkulova, and N. M. Turlybekova, "Development of transport infrastructure of Kazakhstan: problems and prospects," *Kazakh National University Bulletin*, 2015. https://articlekz.com/article/15365

[21] M. Shmulevich, "Transport Infrastructure of Russia's Oil and Gas Industry," *Transport of the Russian Federation. Journal of Science, Practice, Economics*, no. 6 (73), 2017. https://cyberleninka.ru/article/n/transportnaya-infrastruktura-neftegazovoy-otrasli-rossii

[22] M. Lawrence, S. Melibaeva, R. Bullock, and J. Moose, "Caucasus Transport Corridor for Oil and Oil Products," Washington D.C., 2008. https://openknowledge.worldbank.org/handle/10986/12309?show=full

[23] Eurostat, "Crude oil imports by country of origin, EU-28, 2000-2018 (million tonnes)," 2020. https://ec.europa.eu/eurostat/statistics-explained/index.php?title=File:Crude_oil_imports_by_country_of_origin,_EU-27,_2000-2018_(million_tonnes)_F.png

[24] Eurostat, "Crude_oil_imports_by_country_of_origin,_EU-28,_2000-2017_(million_tonnes).png," nrg_ti_oil, 2020. https://ec.europa.eu/eurostat/statistics-explained/images/f/f2/Crude_oil_imports_by_country_of_origin%2C_EU-28%2C_2000-2017_%28million_tonnes%29.png

[25] Eurostat, "Extra-EU_imports_of_petroleum_oil_from_main_trading_partners,_2018_and_2019.png," 2020. https://ec.europa.eu/eurostat/statistics-explained/index.php?title=File:Extra-EU_imports_of_petroleum_oil_from_main_trading_partners,_2018_and_2019_v2.png

[26] P. Argus, "Argus Рынок Каспия," Riga, Latvia, 2017. https://www.argusmedia.com/-/media/Files/sample-reports/argus-russian-caspian-markets.ashx?la=ru&hash=637F3B56CECA9F666573E8BFF91D09BB675C2284

[27] The National Energy Report Lazenergy 2021, Ministry of Energy of the Rebulic of Kazakhstan, October 2021. https://www.kazenergy.com/upload/document/energy-report/NationalReport21_en.pdf

ACTA TECHNICA JAURINENSIS
Vol. 16, No. 3, pp. 123-128, 2023
10.14513/actatechjaur.00706

Thermal and thermomechanical properties of boron nitride-filled acrylonitrile butadiene styrene (ABS) composites

László Lendvai[1,*], Daniele Rigotti[1]

[1]Department of Industrial Engineering, University of Trento
38123 Trento, Italy
*e-mail: lendvai.laszlo@sze.hu

Submitted: 23/06/2023 Accepted: 24/07/2023 Published online: 25/07/2023

Abstract: The present study aims at investigating the effect of hexagonal boron nitride (hBN) nanoplatelets on the properties of acrylonitrile butadiene styrene (ABS) polymer. Composites containing 0-30 vol% hBN were prepared through batchwise melt compounding, which was followed by compression molding. Subsequently, the thermal and thermomechanical properties of the fabricated samples were investigated. The dynamic mechanical analysis (DMA) revealed that the storage modulus of the samples was markedly improved in the entire examined temperature range, while the glass transition temperature also gradually increased as a function of hBN content. According to the thermogravimetric analysis (TGA), the incorporated boron nitride particles enhanced the thermal stability of ABS composites, exhibiting a notably higher decomposition onset temperature. Additionally, the thermal conductivity of the ABS/hBN composites significantly increased by 570% when the hBN content was 30 vol%.

Keywords: acrylonitrile butadiene styrene; boron nitride; thermal conductivity; thermogravimetric analysis, dynamic mechanical analysis

I. INTRODUCTION

Recent times have seen a miniaturization and functionalization in the field of electronic devices [1-3]. One of the major challenges of this trend is to provide effective heat dissipation for the respective products in order to prevent their heat accumulation. Overheating might lead to a reduced lifespan and reliability of such high power density electronic components, including LEDs, Li-ion batteries, microelectronic packaging, and solar cells [4, 5]. One of the most common and cheapest materials for such purposes are polymers owing to their low density, good electrical insulation, and simple processability, however, their use is mostly limited to protective coatings and insulating layers because of their inherently low thermal conductivity, which is typically below 0.5 W/mK [6].

In order to overcome this shortcoming of polymers, a commonly followed strategy is to pair them with thermally conductive fillers [7]. The most commonly applied thermal conductors to incorporate into polymers are metallic, carbonaceous, and ceramic materials. Metals and carbon-based fillers provide an optimal solution when the electrical insulation is not important, albeit, when it is essential along with outstanding heat conductivity, then ceramic additives are the obvious choice since the previous types usually own high electrical conductivity too [8, 9]. Among ceramics, the most common ones to be embedded into polymers to achieve the desired properties are aluminum nitride (AlN), aluminum oxide (Al_2O_3), silica carbides (SiC), and boron nitrides [6]. Oftentimes, researchers aim to improve the interfacial affinity of these particles through functionalization, or else the lack of active groups would result in these particles clumping together and distributing poorly within the polymer matrix [10]. These approaches, however, besides inserting an additional step into the processing sequence are also rather time- and money-intensive procedures.

Hexagonal boron nitride (hBN) nanoplatelets are 2D materials that attracted considerable scientific interest as fillers for various polymers due to the fact that they exhibit several benefits over carbonaceous and metallic particles. The thermal conductivity of hBN is anisotropic because of its layered structure. Accordingly, its in-plane thermal conductivity greatly differs from the through-plane conductivity. The previous one is roughly 600 W/mK because of the strong covalent bonds between B and N atoms, while the latter one is between 1.5 and 2.5 W/mK [11]. Besides their excellent heat conductivity, their major advantages are the outstanding electrical insulation, corrosion resistance, and high thermal stability [10]. Therefore, a large body of work has been devoted to the development of boron nitride-filled polymer composites of improved thermal conductivity throughout the last several years with various thermoplastics and thermosets used as matrix materials. Among others, polypropylene [12], polyamide 6 [13], high density polyethylene [7], and epoxy [14-16] were successfully paired with this innovative ceramic filler.

In this work, a batchwise melt mixing procedure was employed to fabricate hBN-filled acrylonitrile butadiene styrene (ABS)-based polymer composites with enhanced thermal properties. The prepared ABS/hBN samples were subjected to dynamic mechanical analysis to study their thermomechanical behavior and glass transition temperature, while the thermal stability was examined by means of thermogravimetric analysis. Furthermore, the enhancement in the thermal conductivity of ABS as a function of boron nitride content was studied by laser flash technique.

II. Materials and Methods

1. Materials

The ABS polymer (Magnum 3453) used as matrix material was obtained from Trinseo (Wayne, Pennsylvania, USA). The hexagonal boron nitride nanoplatelets under the brand Hebofill 482 were purchased from Henze BNP (Lauben, Germany). The density of hBN is 1.88 g/cm^3 and its average particle size is <30 μm according to its official datasheet. It has to be noted, that this latter value refers to the size of hBN agglomerates, while the individual particles are much smaller than that. Scanning electron microscopic image of the hBN particles is shown in **Fig.1**.

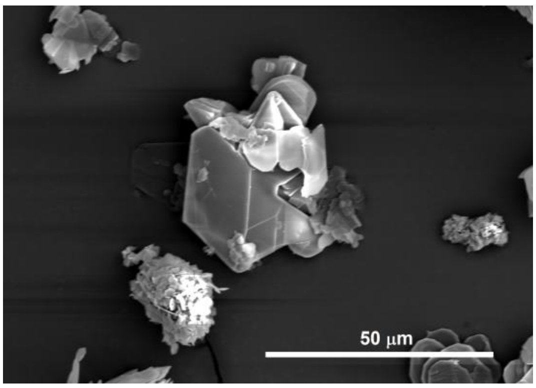

Figure 1. *Scanning electron microscopic image of the applied boron nitride nanoplatelets*

Table 1. *Composition and designation of the prepared samples*

Designation	*ABS-content [vol%]*	*hBN-content [vol%]*
ABS	100	0
ABS_1hBN	99	1
ABS_3hBN	97	3
ABS_5hBN	95	5
ABS_10hBN	90	10
ABS_20hBN	80	20
ABS_30hBN	70	30

2. Preparation of the ABS/hBN composites

The melt mixing process of ABS and hBN was performed with a Haake Polylab internal mixer (Vreden, Germany) equipped with a chamber of 50 cm^3. The compounding was carried out at a temperature of 190 °C, whereas the rotational speed of the mixing elements was 60 rpm. The procedure lasted for 10 minutes with ABS being the first material to be added into the mixer. Subsequently, after 3 minutes the hBN particles were also introduced. This way, ABS-based samples containing 0, 1, 3, 5, 10, 20, and 30 vol% hBN were prepared. The composition and designation of the prepared samples are collected in **Table 1**.

The fabricated samples were compression molded following the melt compounding. This way, sheets of ~2 mm thickness were prepared with a Carver hot press 4122 (Wabash, Indiana, USA) compression molding machine at 190 °C.

3. Characterization

Dynamic mechanical analysis (DMA) was performed with a TA Instruments Q800 device (New Castle, Delaware, USA) in the temperature range of 30 °C to 150 °C with a heating rate of 3 °C/min. The experiments were carried out using a single cantilever clamp. The frequency was 1 Hz and the strain amplitude was set to 0.02%.

Thermogravimetric analysis (TGA) was carried out with a TA Instruments Q500 device (New Castle, Delaware, USA). Samples in the range of 5-10 mg were exposed to a heating program ranging from 30 °C up to 700 °C at a linear heating rate of 10 °C/min in a nitrogen atmosphere.

The enhancement in the thermal conductivity of the samples was determined with a Netzsch LFA 467 Hyperflash (Selb, Germany) light flash apparatus. Round samples with a diameter of 12.7 mm were cut from the compression molded sheets and coated with graphite. Five pulses were performed on each specimen. The thermal conductivity enhancement

(Φ) was determined according to Equation (1) as follows [17]:

$$\Phi = \frac{k_c - k_{ABS}}{k_{ABS}} \times 100\% \qquad (1)$$

where k_c and k_{ABS} represent the thermal conductivity of the composite and the unfilled ABS polymer, respectively.

III. Results and Discussion

1. Dynamic mechanical properties

The dynamic mechanical behavior of the fabricated samples was analyzed in the temperature range of 30 °C to 150 °C. **Fig. 2** shows the temperature dependence of the storage modulus (*E'*) and loss factor (*tan δ*) of the prepared samples. According to **Fig. 2a**, all the composites containing hBN particles exhibited considerably higher storage modulus than that of unfilled ABS in the whole analyzed temperature range. This increment can be explained by the high rigidity of ceramics particles (such as hBN), which confers a general increase in the stiffness of the composite matrix. Meanwhile, the *E'* of all the prepared samples reduced with increasing temperature. At low temperatures, the amorphous part of polymers tends to be in a so-called glassy state. In the glassy state, the motion of chain molecules is restricted, resulting in high storage modulus values that only slightly decrease as a function of temperature. When exceeding the glass transition temperature (T_g) a sudden drop in storage modulus can be observed, representing the transition of the material from the glassy state into a rubber-like state. As seen in **Fig. 2a**, the decrease in storage modulus when exceeding the T_g was highest for those composite samples that contained the highest amount of hBN filler (note the logarithmic scale).

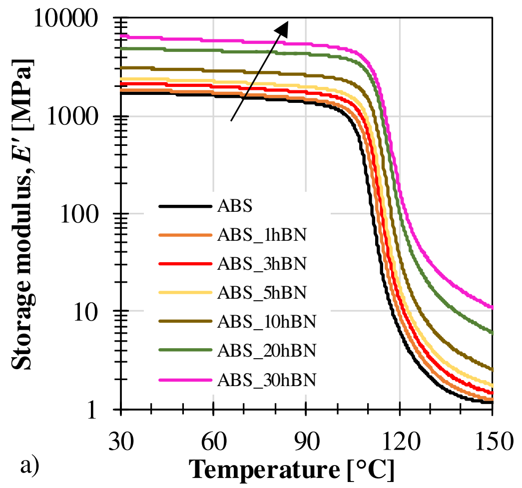

a)

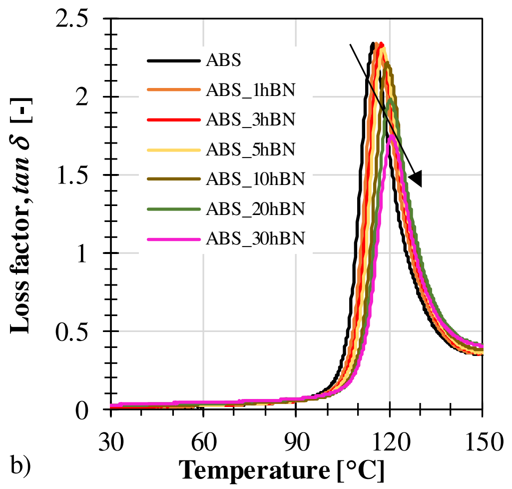

b)

Figure 2. *Storage modulus (a) and loss factor (b) versus temperature of pure ABS compared with composites containing different amounts of hBN*

The temperature dependence of the loss factor is shown in **Fig. 2b**. The glass transition temperature of polymeric materials is mostly defined as the temperature where the *tan δ* curve peaks. Apparently, with increasing hBN content, the T_g of ABS (114.8 °C) shifted towards higher temperatures, reaching 120.8 °C when the maximum of 30 vol% hBN was incorporated into the matrix. This shift to higher temperatures refers to a reduced chain mobility of the ABS molecules in the presence of hBN [18]. Additionally, it can be seen that the *tan δ* peaks declined with the introduction of ceramic particles indicating a reduced damping capacity of the ABS polymer.

2. TGA behavior

The thermal stability of the samples was analyzed by means of TGA measurements. The TGA thermograms of unfilled ABS and the composites against the increasing temperature are illustrated in **Fig. 3a**, whereas **Fig. 3b** shows their derivatives (DTG). Clearly, all samples exhibited a single-step degradation process, corresponding to the decomposition of macromolecular chains of ABS polymer. The degradation manifested in a sudden drop in the TGA thermograms (**Fig. 3a**) and in a sharp peak in the DTG curves (**Fig. 3b**). The thermal stability of the fabricated samples was analyzed in the form of the onset temperature and maximum thermal degradation temperature. The onset of the decomposition (T_o) was considered as the temperature where the specimens suffered 5% of weight loss, while the temperature of the maximum degradation (T_p) was determined based on the peak points of the DTG curves. The T_o value of neat ABS was 381.8 °C, which gradually improved with increasing hBN content, reaching the highest temperature of 391.1 °C for the ABS_30hBN sample. This enhancement in thermal stability can be attributed to the high heat capacity of the hBN filler, which is embedded into the ABS matrix.

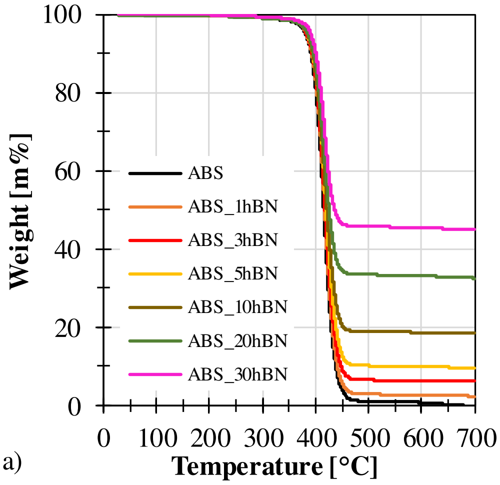

a)

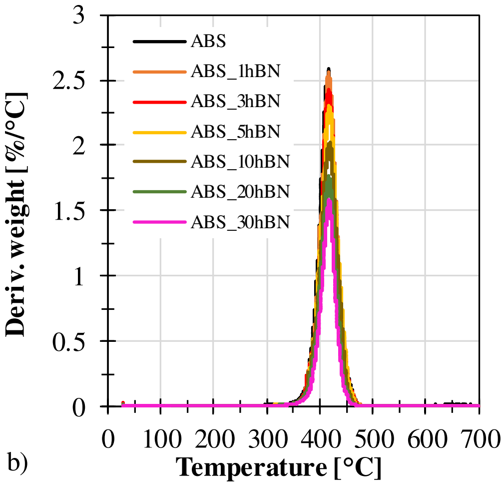

b)

Figure 3. *Thermograms of TGA (a) and DTG (b) versus temperature of pure ABS compared with composites containing different amounts of hBN*

Meanwhile, the ceramic fillers did not significantly affect the T_p values. The temperature corresponding to the maximum degradation was the lowest for unfilled ABS (416.5 °C), but it only increased slightly in the presence of boron nitride particles, with all the composites being in the small temperature range of 416.6 and 418.6 °C.

3. Thermal conductivity

The thermal conductivity enhancement data of all hBN-containing composites relative to that of unfilled ABS are depicted in **Fig. 4**. The thermal conductivity of commercial ABS was determined as 0.19 W/mK, which is in good agreement with the literature [6]. As expected, with hBN nanoplatelets getting incorporated into the polymer matrix, the thermal conductivity of ABS increased simultaneously. The relative enhancement of thermal conductivity was 2.5%, 5.8%, 45.3%, 101.5%, 263.5%, and 572.0% for the composites

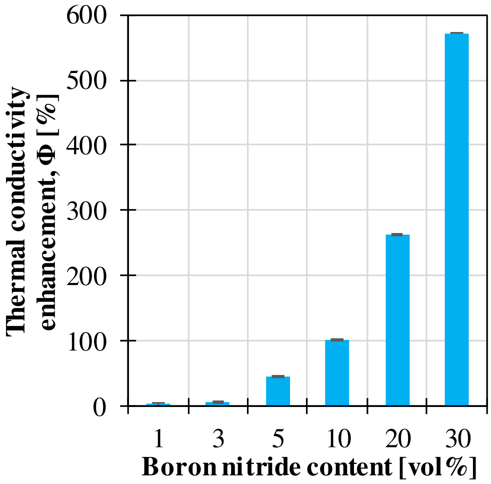

Figure 4. *Thermal conductivity enhancement of ABS at various hBN concentrations*

containing 1, 3, 5, 10, 20, and 30 vol% of boron nitride particles, respectively.

IV. Conclusions

In the present study, ABS/hBN composites were fabricated through batchwise melt compounding using an internal mixer. Subsequently, the composites were formed into sheets through compression molding. The thermomechanical behavior of the fabricated samples was analyzed by means of dynamic mechanical analysis. It was revealed that the hBN particles greatly enhance the storage modulus of ABS in the whole examined temperature range while also increasing its glass transition temperature prominently. Through thermogravimetric analysis it was shown that the onset temperature of ABS shifts to a higher temperature if hBN nanoplatelets are incorporated into it, referring to an improved thermal stability. Additionally, the laser flash measurement verified that this type of ceramic filler is highly efficient in increasing the thermal conductivity of ABS polymer, reaching a maximum relative increment of 570% at 30 vol% hBN concentration.

Overall, this study provides solid evidence about all the investigated properties of ABS being markedly improved in the presence of hBN particles.

Acknowledgment

L. Lendvai is grateful for the support of the Hungarian Eötvös Scholarship of the Tempus Foundation.

AUTHOR CONTRIBUTIONS

L. Lendvai: Conceptualization, Experiments, Fund acquisition, Writing – original draft

D. Rigotti: Conceptualization, Experiments, Writing – review and editing

Disclosure statement

The authors declare that they have no known competing financial interests or personal relationships that could have appeared to influence the work reported in this paper.

References

[1] J. V. Bondareva, D. Chernodubov et al., Thermal and Electrical Properties of Additively Manufactured Polymer–Boron Nitride Composite, Polymers 15 (5) (2023) 1214. https://doi.org/10.3390/polym15051214

[2] Y. Cui, F. Xu et al., Construction of 3D interconnected boron nitride/carbon nanofiber hybrid network within polymer composite for thermal conductivity improvement, Journal of Materials Science & Technology 147 (2023) pp. 165-175. https://doi.org/10.1016/j.jmst.2022.10.077

[3] K. Li, Y. Liu et al., Construction of 3D framework of BN and silica with advanced thermal conductivity of epoxy composites, Journal of Polymer Research 30 (6) (2023) 219. https://doi.org/10.1007/s10965-023-03589-7

[4] B. Almuallim, W. S. W. Harun et al., Thermally conductive polymer nanocomposites for filament-based additive manufacturing, Journal of Materials Science 57 (6) (2022) pp. 3993-4019. https://doi.org/10.1007/s10853-021-06820-2

[5] W. Wu, M. Zheng et al., Thermally conductive composites based on hexagonal boron nitride nanosheets for thermal management: Fundamentals to applications, Composites Part A: Applied Science and Manufacturing 169 (2023) 107533. https://doi.org/10.1016/j.compositesa.2023.107533

[6] A. Khan, M. Puttegowda et al., Review on nitride compounds and its polymer composites: a multifunctional material, Journal of Materials Research and Technology 18 (2022) pp. 2175-2193. https://doi.org/10.1016/j.jmrt.2022.03.032

[7] S.-N. Wei, L. Xin et al., A study of the mechanical performance of nanocomposites of polyethylene containing exfoliated boron nitride nanoplatelets, Polymer Composites 43 (9) (2022) pp. 6276-6286. https://doi.org/10.1002/pc.26936

[8] H. Peidayesh, K. Mosnáčková et al., Thermoplastic Starch–Based Composite Reinforced by Conductive Filler Networks: Physical Properties and Electrical Conductivity Changes during Cyclic Deformation, Polymers, 13 (21) (2021) 3819. https://doi.org/10.3390/polym13213819

[9] A. Boudenne, L. Ibos et al., Electrical and thermal behavior of polypropylene filled with copper particles, Composites Part A: Applied Science and Manufacturing, 36 (11) (2005) pp. 1545-1554. https://doi.org/10.1016/j.compositesa.2005.02.005

[10] W. Han, X. Chu et al., Anchoring modified polystyrene to boron nitride nanosheets as highly thermal conductive composites for heat dissipation, Polymer Composites 43 (3) (2022) pp. 1844-1851. https://doi.org/10.1002/pc.26502

[11] C. Pan, J Zhang et al., Investigation of the through-plane thermal conductivity of polymer composites with in-plane oriented hexagonal boron nitride, International Journal of Heat and Mass Transfer 120 (2018) pp. 1-8. https://doi.org/10.1016/j.ijheatmasstransfer.2017.12.015

[12] W. Cheewawuttipong, D. Fuoka et al., Thermal and Mechanical Properties of Polypropylene/Boron Nitride Composites, Energy Procedia 34 (2013) pp. 808-817. https://doi.org/10.1016/j.egypro.2013.06.817

[13] H.-X. Zhang, D. H. Seo et al., Fabrication of highly thermal conductive PA6/hBN composites via in-situ polymerization process, Journal of Polymer Research 28 (2) (2021) 42. https://doi.org/10.1007/s10965-020-02378-w

[14] Z. Wang, X. Wang, et al., Preparation of a 3D BN network structure by a salt-template-assisted method filled with epoxy resin to obtain high thermal conductivity nanocomposites, Polymer Composites 44 (6) (2023) pp. 3610-3621. https://doi.org/10.1002/pc.27348

[15] D. R. Salunke, V. Gopalan, Thermal and Electrical behaviors of Boron Nitride/Epoxy reinforced polymer matrix composite—A review, Polymer Composites 42 (4) (2021) pp. 1659-1669. https://doi.org/10.1002/pc.25952

[16] X. Wu, W. Liu et al., Constructing three-dimensional boron nitride network for highly thermally conductive epoxy resin composites, Polymer Composites 43 (3) (2022) pp. 1711-1717.

ORCID

L. Lendvai https://orcid.org/0000-0003-3670-327X

D. Rigotti https://orcid.org/0000-0002-2337-8669

https://doi.org/10.1002/pc.26490

[17] W. Li, Z. Song et al., Largely enhanced dielectric and thermal conductive properties of novel ternary composites with small amount of nanofillers, Composites Science and Technology 163 (2018) pp. 71-80. https://doi.org/10.1016/j.compscitech.2018.05.008

[18] K.-H. Su, C.-Y. Su et al., Improvement of the Thermal Conductivity and Mechanical Properties of 3D-Printed Polyurethane Composites by Incorporating Hydroxylated Boron Nitride Functional Fillers, Materials 16 (1) (2023) 356. https://doi.org/10.3390/ma16010356